1834 *Inorg. Chem.* **2010**, *49*, 1834–1848
DOI: 10.1021/ic9021855

Inorganic Chemistry
Article

Heterobimetallic Metal-Complex Assemblies Constructed from the Flexible Arm-Like Ligand 1,1′-Bis[(3-pyridylamino)carbonyl]ferrocene: Structural Versatility in the Solid State

Kai-Ju Wei,*,† Jia Ni,† and Yangzhong Liu*,†

†*Department of Chemistry, University of Science & Technology of China, Hefei 230026, P.R. China*

Received November 7, 2009

The bidentate ferrocenyl sandwich molecule 1,1′-bis[(3-pyridylamino)carbonyl]ferrocene (**3-BPFA**) has been employed as an organometallic ligand in reactions with a series of transition metal salts to construct heterobimetallic architectures. X-ray crystallographic characterization reveals that the crystal packing of free ligand 3-BPFA induces spontaneous resolution of helical chains via intermolecular hydrogen bonds. By combining the flexibility from the arm-like molecule (**3-BPFA**) with the variation of the coordination property from different metal ions and/or the different counteranions, five different types of architectures are prepared: one octahedral coordination cage (copper(II) complex **1**); two discrete pseudocapsules for combination of chlorine anions (nickel(II) complex **2** and cobalt(II) complex **3**); two dimers with metal−metal interactions (silver(I) complexes **4** and **5**); one macrocyclic complex (mercury(II) complex **6**); and five two-dimensional mixed-metal-organic frameworks (M′-MOFs) (zinc(II), cadmium(II), and mercury(II) complexes **7**−**11**). The structures of all complexes are characterized in detail by IR, elementary analysis, and single-crystal X-ray diffraction analysis. The factors inducing the structure variation among the complexes are discussed by taking account of the coordination geometry of different metal ions, the span angle between the two "arms", and the coordination mode of the 3-BPFA ligand.

Introduction

The self-assembly of small "building blocks" with transition metal ions to generate cages, capsules, macrocycles, helixes, networks, and other supramolecular architectures is a major area of research in supramolecular chemistry, materials chemistry, and crystal engineering.[1] The rational design and the synthesis of these charming architectures are essential for the creation of new functional materials with solvent-inclusion or gas-adsorption characteristics or with special optical, electronic, magnetic, and catalytic properties.[2] One straightforward strategy to construct these assemblies is to use metal "nodes" and organic "spacers" to form the primary structure by coordination bonds in cooperation with weak noncovalent interactions, such as H-bonding and π stacking, to organize these primary structures into supramolecular architectures.[3] The research mainly focuses on homometallic systems. Heterometallic complexes, which often exhibit novel electromagnetic properties, remain relatively scarce because

*To whom correspondence should be addressed. E-mail: kjwei@ustc.edu.cn (K.-J.W.), liuyz@ustc.edu.cn (Y.L.). Fax: +86-551-3600874.

(1) (a) Sunmby, C. J.; Fisher, J.; Prior, T. J.; Hardie, M. J. *Chem.—Eur. J.* **2006**, *12*, 2945–2959. (b) Amouri, H.; Desmarets, C.; Bettoschi, A.; Rager, M. N.; Boubekeur, K.; Rabu, P.; Drillon, M. *Chem.—Eur. J.* **2007**, *13*, 5401–5407. (c) Salazar-Mendoza, D.; Guerrero-Alvarez, J.; Hőpfl, H. *Chem. Commun.* **2008**, 6543–6545. (d) Biros, S. M.; Yeh, R. M.; Raymond, K. N. *Angew. Chem., Int. Ed.* **2008**, *47*, 6062–6064. (e) Suzuki, K.; Iida, J.; Sato, S.; Kawano, M.; Fujita, M. *Angew. Chem., Int. Ed.* **2008**, *47*, 5780–5782. (f) Hiraoka, S.; Sakata, Y.; Shionoya, M. *J. Am. Chem. Soc.* **2008**, *130*, 10058–10059. (g) Dalgarno, S. J.; Power, N. P.; Atwood, J. L. *Coord. Chem. Rev.* **2008**, *252*, 825–841. (h) Kumar, A.; Sun, S.-S.; Lees, A. J. *Coord. Chem. Rev.* **2008**, *252*, 922–939. (i) Steel, P. J.; Fitchett, C. M. *Coord. Chem. Rev.* **2008**, *252*, 990–1006. (j) Fox, O. D.; Cookson, J.; Wilkinson, E. J. S.; Drew, M. G. B.; MacLean, E. J.; Teat, S. J.; Beer, P. D. *J. Am. Chem. Soc.* **2006**, *128*, 6990–7002. (k) Seidel, S. R.; Stang, P. J. *Acc. Chem. Res.* **2002**, *35*, 972–983. (l) Hao, X.-R.; Wang, X.-L.; Qin, C.; Su, Z.-M.; Wang, E.-B.; Lan, Y.-Q.; Shao, K.-Z. *Chem. Commun.* **2007**, 4620–4622. (m) Cui, Y.; Lee, S. J.; Lin, W. *J. Am. Chem. Soc.* **2003**, *125*, 6014–6015. (n) Pantos, G. D.; Pengo, P.; Sanders, J. K. M. *Angew. Chem., Int. Ed.* **2007**, *46*, 194–197. (o) Yao, Q.-X.; Xuan, W.-M.; Zhang, H.; Tu, C.-Y.; Zhang, J. *Chem. Commun.* **2009**, 59–61. (p) Hess, C. R.; Weyhermüller, T.; Bill, E.; Wieghardt, K. *Angew. Chem., Int. Ed.* **2009**, *48*, 3703–3706. (q) Kasai, K.; Sato, M. *Chem. Asian J.* **2006**, *1*, 344–348. (r) Fromm, K. M. *Coord. Chem. Rev.* **2008**, *252*, 856–885. (s) Tranchemontagne, D. J.; Ni, Z.; Keeffe, M. O.; Yaghi, O. M. *Angew. Chem., Int. Ed.* **2008**, *47*, 2–14. (t) Nohra, B.; Rodriguez-Sanz, E.; Lescop, C.; Réau, R. *Chem.—Eur. J.* **2008**, *14*, 2034–2047. (u) Zangrando, E.; Casanova, M.; Alessio, E. *Chem. Rev.* **2008**, *108*, 4979–5013.

(2) (a) Yamada, T.; Kitagawa, H. *J. Am. Chem. Soc.* **2009**, *131*, 6312–6313. (b) Lee, S. J.; Lin, W. *Acc. Chem. Res.* **2008**, *41*, 521–537. (c) Galli, S.; Masciocchi, N.; Tagliabue, G.; Sironi, A.; Navarro, J. A. R.; Salas, J. M.; Mendez-Liñan, L.; Domingo, M.; Perez-Mendoza, M.; Barea, E. *Chem.—Eur. J.* **2008**, *14*, 9890–9901. (d) Pang, J.; Marcotte, E. J. P.; Seward, C.; Brown, R. S.; Wang, S. N. *Angew. Chem., Int. Ed.* **2001**, *40*, 4042–4045. (e) Seward, C.; Jia, W. L.; Wang, R. Y.; Enright, G. D.; Wang, S.-N. *Angew. Chem., Int. Ed.* **2004**, *43*, 2933–2937.

(3) (a) Su, C.-Y.; Goforth, A. M.; Smith, M. D.; zur Loye, H.-C. *Inorg. Chem.* **2003**, *42*, 5685–5692. (b) Wu, G.; Wang, X.-F.; Okamura, T.; Sun, W.-Y.; Ueyama, N. *Inorg. Chem.* **2006**, *45*, 8523–8532.

Published on Web 01/22/2010

of the coordinative complexity of the heterometallic ions involved in the self-assembly process.[4]

Organometallic ligands, as "building blocks" to link other metal ions for extending organic units, have proved to be ideal candidates for hierarchical assembly into heterometallic supramolecular architectures.[5] Ferrocene with the free rotational center, as an important member of this family, has shown the fundamental and practical implications in materials science, organic synthesis, and catalysis.[6] Several research groups[7] have reported the synthesis of ferrocene-based bidentate ligands containing pyridine and rigid or flexible "spacers", including -C≡C-, -C=C-, -N=C-, -Ph-, -CH_2-, -S-, -CONH-. Their relevant coordination compounds have also been studied for the possibility of exploiting their properties in various appplications, such as chemical sensing,[8] nonlinear optical properties,[9] and ion or molecule recognition.[10] A number of novel structures have been constructed in this process, such as macrocycles, cages, and helices.[5d,9,11] However, to our knowledge, there is no systematic research on the construction of heterometallic superstructures by using sandwich-type organometallic molecule as a "building block", in which the different metal ions and/or counteranions may rationally hold the rotation of the sandwich.

On the other hand, flexible organic "spacers" are relatively less predictable in self-assembly and are inclined to form oligomers or low-dimensional polymers, such as cages, macrocycles, and helicates upon their reactions with transition metal ions.[9,11,12] Additionally, incorporating flexible "spacers" in supramolecular systems may generate flexible assemblies, in which the bridging ligands could adapt a more thermo-dynamically stable conformation for host-guest interactions. On this aspect, the amide functional group is an outstanding example of flexible "spacers", which can form strong intra- or intermolecular hydrogen bonds because of the simultaneous presence of amide N−H groups (H-bond donor) and amide oxygen atoms (H-bond acceptor).

Encouraged by these findings and intrigued by the possibility of using arm-like linkers based on ferrocene moiety to achieve novel heterometallic supramolecular architectures, a ditopic molecule 1,1′-bis[(3-pyridylamino)carbonyl]ferrocene (3-BPFA), combining the amide flexibility and organometallic functionality, has been designed and synthesized.[13]

The 3-BPFA molecule is capable, to a certain extent, of adjusting itself sterically owing to the flexibility of "arm" units. Each pyridyl group in 3-BPFA is linked by a C−N bond, which allows rotation about the single bond. This rotation leads to the conformational change of 3-BPFA, so that this arm-like ligand possesses conformation flexibility (Scheme 1). Because of the different coordination geometry requirements, metal ions can be employed as angular directional units. Therefore, the incorporation of the flexibility of arm-like bridging ligand with coordination variation of metal ions, the bimetal-complex assembly offers structural advantages for solid-state functional materials. In view of the flexibility of the two Cp−"arm" units, since each Cp ring can rotate round the Fe center freely, 3-BPFA can adopt various conformations (cisoid, transoid, and intermediate conformations) upon coordination structures (Scheme 2). In general, the cisoid conformation leads to the formation finite coordination geometries, for example, macrocycles,[5c,7a,9a,14] which greatly depend on the properties of the "arm" spacers. The transoid tends to infinite chains or networks, although such structures have only been rarely reported.[7e,15] The conformation of 3-BPFA adopted in the individual complex

(4) (a) Westerhausen, M. *Dalton Trans*. **2006**, 4755–4768. (b) Zhang, B.; Ni, Z.-H.; Cui, A.-L.; Kou, H.-Z. *New J. Chem*. **2006**, *30*, 1327–1332. (c) Stork, J. R.; Thoi, V. S.; Cohen, S. M. *Inorg. Chem*. **2007**, *46*, 11213–11223. (d) Zhang, Y.; Chen, B.; Fronczek, F. R.; Maverick, A. W. *Inorg. Chem*. **2008**, *47*, 4433–4435. (e) Chen, B.; Fronczek, F. R.; Maverick, A. W. *Inorg. Chem*. **2004**, *43*, 8209–8211. (f) Chen, B.; Fronczek, F. R.; Maverick, A. W. *Chem. Commun*. **2003**, 2166–2167.

(5) (a) Bar, A. K.; Chakrabarty, R.; Mukherjee, P. S. *Organometallics*. **2008**, *27*, 3806–3810. (b) Lozan, V.; Buchhol, A.; Plass, W.; Kersting, B. *Chem.—Eur. J*. **2007**, *13*, 7305–7316. (c) Braga, D.; Polito, M.; D'Addario, D.; Tagliavini, E. *Organometallics*. **2003**, *22*, 4532–4538. (d) Chandrasekhar, V.; Thirumoorthi, R. *Organometallics*. **2007**, *26*, 5415–5422. (e) Yu, S.-Y.; Sun, Q.-F.; Lee, T. K.-M.; Cheng, E. C.-C.; Li, Y.-Z.; Yam, V. W.-W. *Angew. Chem., Int. Ed*. **2008**, *47*, 4551–4554. (f) Chandrasekhar, V.; Gopal, K.; Nalvarajan, S.; Singh, P.; Steiner, A.; Zacchini, S.; Bickley, J. F. *Chem.—Eur. J*. **2005**, *11*, 5437–5448. (g) Braga, D.; Maini, L.; Giaffreda, S. L.; Grepioni, F.; Chierotti, M. R.; Gobetto, R. *Chem.—Eur. J*. **2004**, *10*, 3261–3269. (h) Venkatasubbaiah, K.; DiPasquale, A. G.; Bolte, M.; Rheingold, A. L.; Jäkle, F. *Angew. Chem*. **2006**, *118*, 6992–6995.

(6) (a) van Staveren, D. R.; Metzler-Nolte, N. *Chem. Rev*. **2004**, *104*, 5931–5985. (b) Dai, L.-X.; Tu, T.; You, S.-L.; Deng, W.-P.; Hou, X.-L. *Acc. Chem. Res*. **2003**, *36*, 695–667. (c) Martķnez, R.; Ratera, I.; Tárraga, A.; Molina, P.; Veciana, J. *Chem. Commun*. **2006**, 3809–3811. (d) Peris, E. *Coord. Chem. Rev*. **2004**, *248*, 279–297. (e) Fujimoto, K.; Kawai, H.; Amano, M.; Inouye, M. *J. Org. Chem*. **2008**, *73*, 5123–5126.

(7) (a) Lindner, E.; Zong, R.; Eichele, K.; Weisser, U.; Ströbele, M. *Eur. J. Inorg. Chem*. **2003**, 705–712. (b) Chebny, V. J.; Dhar, D.; Lindeman, S. V.; Rathore, R. *Org. Lett*. **2006**, *8*, 5041–5044. (c) Broderick, E. M.; Diaconescu, P. L. *Inorg. Chem*. **2009**, *48*, 4701–4706. (d) Weidner, T.; Ballav, N.; Zharnikov, M.; Priebe, A.; Long, N. J.; Maurer, J.; Winter, R.; Rothenberger, A.; Fenske, D.; Rother, D.; Bruhn, C.; Fink, H.; Siemeling, U. *Chem.—Eur. J*. **2008**, *14*, 4346–4360. (e) Gao, Y.; Twamley, B.; Shreeve, J. M. *Organometallics*. **2006**, *25*, 3364–3369. (f) Moriuchi, T.; Ikeda, I.; Hirao, T. *Organometallics*. **1995**, *14*, 3578–3580. (g) Beer, P. D.; Hayes, E. J. *Coord. Chem. Rev*. **2003**, *240*, 167–189. (h) Peris, E. *Coord. Chem. Rev*. **2004**, *248*, 279–297.

(8) (a) Tomapatanaget, B.; Tuntulani, T.; Chailapakul, O. *Org. Lett*. **2003**, *5*, 1539–1542. (b) Li, M.; Cai, P.; Duan, C.; Lu, F.; Xie, J.; Meng, Q. *Inorg. Chem*. **2004**, *43*, 5174–5176. (c) Zhang, D.; Zhang, Q.; Su, J.; Tian, H. *Chem. Commun*. **2009**, 1700–1702.

(9) (a) Li, G.; Song, Y.; Hou, H.; Li, L.; Fan, Y.; Zhu, Y.; Meng, X.; Mi, L. *Inorg. Chem*. **2003**, *42*, 913–920. (b) Li, L. K.; Song, Y. L.; Hou, H. W.; Fan, Y. T.; Zhu, Y. *Eur. J. Inorg. Chem*. **2005**, 3238–3249. (c) Wu, J.; Song, Y.; Zhang, E.; Hou, H.; Fan, Y.; Zhu, Y. *Chem.—Eur. J*. **2006**, *12*, 5823–5831.

(10) (a) Beer, P. D. *Acc. Chem. Res*. **1998**, *31*, 71–80. (b) Beer, P. D.; Graydon, A. R.; Johnson, A. O. M.; Smith, D. K. *Inorg. Chem*. **1997**, *36*, 2112–2118. (c) Beer, P. D.; Davis, J. J.; Drillsma-Milgrom, D. A.; Szemes, F. *Chem. Commun*. **2002**, 1716–1717. (d) Niu, H.-T.; Yin, Z.; Su, D.; Niu, D.; Ao, Y.; He, J.; Cheng, J.-P. *Tetrahedron*. **2008**, *64*, 6300–6306. (e) Caballero, A.; Espinosa, A.; Tárraga, A.; Molina, P. *J. Org. Chem*. **2008**, *73*, 5489–5497. (f) Otón, F.; Espinosa, A.; Tórraga, A.; De Arellano, C. R.; Molina, P. *Chem.—Eur. J*. **2007**, *13*, 5742–5752. (g) Bondy, C. R.; Loeb, S. J. *Coord. Chem. Rev*. **2003**, *240*, 77–99.

(11) (a) Fang, C. J.; Duan, C. Y.; He, C.; Meng, Q. J.; Wang, Z. M.; Yan, C. H. *Chem . Commun*. **2001**, 2540–2541. (b) Fang, C. J.; Duan, C.-Y.; Mo, H.; He, C.; Meng, Q.-J.; Liu, Y.-J.; Mei, Y.-H.; Wang, Z.-M. *Organometallic*. **2001**, *20*, 2525–2532. (c) Fang, C. J.; Duan, C. Y.; He, C.; Meng, Q. J. *Chem . Commun*. **2000**, 1187–1188. (d) Li, X.; Liu, W.; Zhang, H.-Y.; Wu, B.-L. *J. Organomet. Chem*. **2008**, *693*, 3295–3302.

(12) (a) Burchell, T. J.; Eisler, D. J.; Puddephatt, R. J. *Inorg. Chem*. **2004**, *43*, 5550–5557. (b) Paul, R. L.; Argent, S. P.; Jeffery, J. C.; Harding, L. P.; Lynam, J. M.; Ward, M. D. *Dalton Trans*. **2004**, 3453–3458. (c) Han, L.; Hong, M.; Wang, R.; Luo, J.; Liu, Z.; Yuan, D. *Chem. Commun*. **2003**, 2580–2581.

(13) Wei, K.-J.; Ni, J.; Xie, Y.-S.; Liu, Y.; Liu, Q.-L. *Dalton Trans*. **2007**, 3390–3397.

(14) (a) Braga, D.; Polito, M.; Bracaccini, M.; D'Addario, D.; Tagliavini, E.; Proserpio, D. M.; Grepioni, F. *Chem. Commun*. **2002**, 1080–1081. (b) Sadhukhan, N.; Patra, S. K.; Sana, K.; Bera, J. K. *Organometallic*. **2006**, *25*, 2914–2916. (c) Weidner, T.; Ballav, N.; Zharnikov, M.; Priebe, A.; Long, N. J.; Maurer, J.; Winter, R.; Rothenberger, A.; Fenske, D.; Rother, D.; Bruhn, C.; Fink, H.; Siemeling, U. *Chem.—Eur. J*. **2008**, *14*, 4346–4360.

(15) (a) Guo, D.; Zhang, B.; Duan, C.-Y.; Cao, X.; Meng, Q.-J. *Dalton Trans*. **2003**, 282–284. (b) Guo, D.; Mo, H.; Duan, C.-Y.; Lu, F.; Meng, Q.-J. *Dalton Trans*. **2002**, 2593–2594. (c) Kumalah, S. A.; Holman, T. *Inorg. Chem*. **2009**, 48, in press.

Scheme 1. Three Typical Possible Conformations of 3-BPFA without Considering the Rotation of Cp-Rings

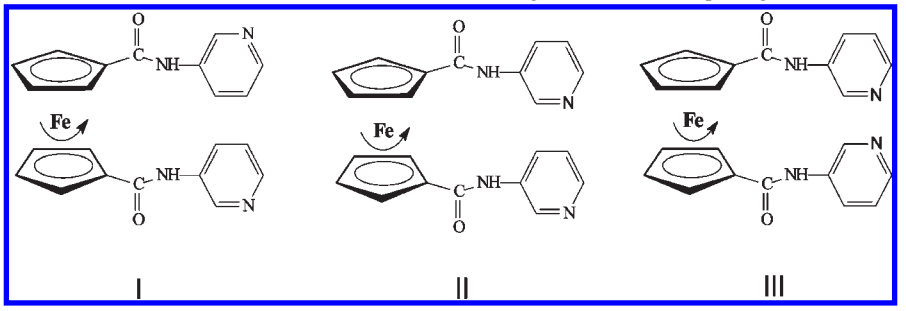

Scheme 2. Two Typical Possible Conformations of 3-BPFA without Considering the Rotation of Py-Rings

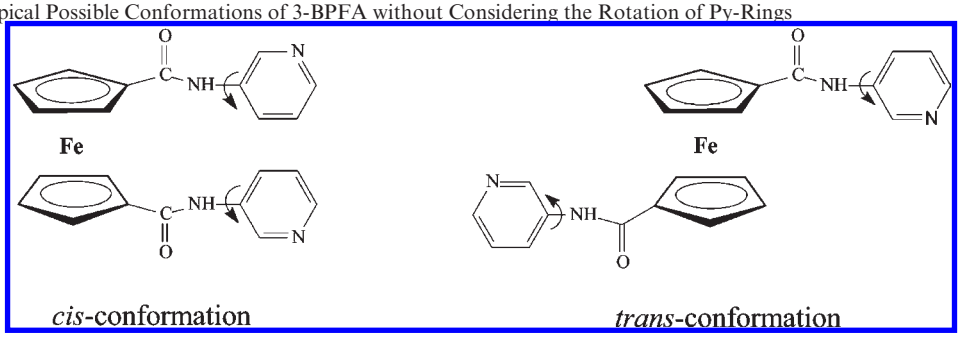

Scheme 3. Schematic Representation of the Assembled Structures of 3-BPFA and Transition Metal Ions

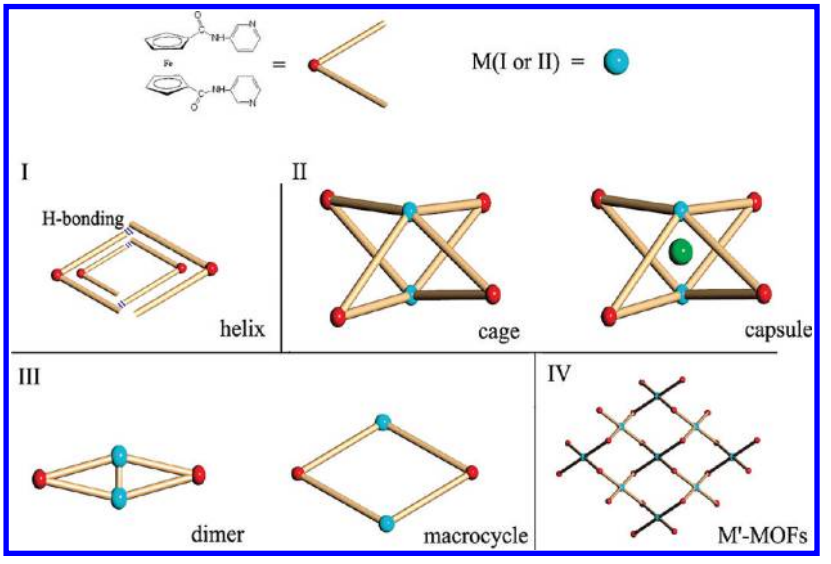

would be potentialy dependent on several effects, for example, the nature of metal cation, the size and polarity of the anion, the template effect of solvent molecule, and other subtle factors.

Considering all relevant effects, it can be envisaged that at least four possible architectures of the self-assemblies can reasonably exist based on this arm-like ligand 3-BPFA: helix or zigzag; cage or capsule; dimer or macrocycle; and mixed-metal-organic frameworks (M′-MOFs) (Scheme 3). The configuration, coordination activity, and relative orientation of the donor groups of the organic spacers in 3-BPFA undoubtedly take pivotal roles in determinning the terminal structure and geometry of the assemblies. First, the amide groups are easy to employ to induce helicity in the superstructures through inter- or intramolecular hydrogen bonding interactions of organic molecule.[16] Second, metal-containing subunits with programmed dihedral angles can be employed for the self-assembly of polyhedral cages, macromolecular polygons, and frameworks. Third, the flexible "arms" can potentially enhance interligand interactions through weak noncovalent interactions, including π stacking and H-bonding, and thereby may maintain the high stability in the final solid-state structure.

In this work, we have performed a systematic investigation of the reaction of 3-BPFA with a variety of Cu^{II}, Ni^{II}, Co^{II}, Ag^{I}, Zn^{II}, Cd^{II}, and Hg^{II} salts with different counteranions. X-ray crystallographic characterization reveals a helical supramolecular array of 3-BPFA by intermolecular N−H···O=C hydrogen bonds. Operating two equivalent flexible

(16) Norsten, T. B.; McDonald, R.; Branda, N. R. *Chem. Commun.* **1999**, 719–720.

"arms" of 3-BPFA through the use of metal ions and/or counteranions, a whole family of heterobimetallic assemblies (complexes **1**−**11**) have been prepared. In copper(II) compound $[Cu_2(3\text{-BPFA})_4(H_2O)_2](ClO_4)_4\cdot 4CH_3OH$ (**1**), four 3-BPFA molecules bridge two copper(II) centers to form a discrete molecular cage. Similarly, nickel(II) and cobalt(II) compounds $[Ni_2(\mu\text{-Cl})(3\text{-BPFA})_4(H_2O)_2](ClO_4)_3$ (**2**) and $[Co_2(\mu\text{-Cl})(3\text{-BPFA})_4(H_2O)_2](ClO_4)_3\cdot 4CH_3OH$ (**3**) also form discrete cage-type assemblies; however, a chlorine anion is combined in the cavity of the molecular sphere via coordination interactions. Silver(I) compounds $[Ag_2(3\text{-BPFA})_2](CF_3SO_3)_2\cdot 3H_2O$ (**4**) and $[Ag_2(3\text{-BPFA})_2](CF_3COO)_2\cdot 2CH_3CN\cdot C_6H_6$ (**5**) exhibit two dimer structures containing Ag−Ag interactions. Mercury(II) compound $[Hg_2(3\text{-BPFA})_2Br_4]$ (**6**) constructs a distorted tetranuclear macrocyclic assembly. Two zinc(II) complexes, $[Zn(3\text{-BPFA})_2(SCN)_2]_n$ (**7**) and $[Zn(3\text{-BPFA})_2(N_3)_2]_n$ (**8**), two cadmium(II) complexes $[Cd(3\text{-BPFA})_2Br_2]_n$ (**9**) and $[Cd(3\text{-BPFA})_2(H_2O)_2]_n(NO_3)_{2n}$ (**10**), and one mercury(II) complex $[Hg(3\text{-BPFA})_2Cl_2]_n$ (**11**) show similar two-dimensional (2D) M′-MOFs. It can be concluded from these compounds that the structural versatility of bimetallic 3-BPFA complexes is caused by the metal-coordination modes and the flexibility of two "arms" in 3-BPFA molecule, in which the rotary angles varies between two "arms" upon different metal coordination. The preliminary results of reaction of 3-BPFA with the Cu^{II}, Ni^{II}, and Co^{II} salts have been reported previously.[13]

Experimental Section

Materials and Physical Measurements. All starting chemicals were of reagent-grade quality, obtained from commercial sources, and used without further purification. Solvents used in reactions were dried by standard procedures. Benzene was freshly distilled over sodium and benzophenone. Dichloromethane was dried and distilled over P_2O_5 under a nitrogen atmosphere.

The FT-IR spectra were recorded in the region 400−4000 cm^{-1} on a Bruker EQUINOX 55 VECTOR22 spectrophotometer: the samples were prepared using KBr pellets. Elementary analyses were carried out with an Elementar Vario EL-III analyzer. UV−visible absorption spectra were recorded on a UV-2401PC spectrophotometer. Electrochemical experiments were performed on CHI 660C Electrochemical Workstation. A Ag/Ag+ (0.1 M $AgNO_3$ in *N*,*N*′-dimethylformamide (DMF) solution) reference electrode was employed and connected to the electrolyte through a salt bridge (0.1 M Bu_4NClO_4 in DMF solution), and the auxiliary electrode was a platinum wire. Ferrocene was used as an external standard. Its potential of 456 mV was determined by a separate differential pulse voltammetric experiment in the DMF solvent, and all potentials in the present paper are reported relative to the Fc/Fc+ standard.

The free ligand 1,1′-bis[(3-pyridylamino)carbonyl]ferrocene (**3-BPFA**) and its coordinated complexes $[Cu_2(3\text{-BPFA})_4(H_2O)_2](ClO_4)_4\cdot 4CH_3OH$ (**1**), $[Ni_2(\mu\text{-Cl})(3\text{-BPFA})_4(H_2O)_2](ClO_4)_3$ (**2**) and $[Co_2(\mu\text{-Cl})(3\text{-BPFA})_4(H_2O)_2](ClO_4)_3\cdot 4CH_3OH$ (**3**), have been prepared as previously reported.[13]

Caution! *Perchlorate salts of metal complexes with organic ligands are potentially explosive! Only small amounts of these materials should be prepared, and they should be handled with great caution.*

Synthesis of $[Ag_2(3\text{-BPFA})_2](CF_3SO_3)_2\cdot 3H_2O$ (4). Upon a solution of 3-BPFA (0.0426 g, 0.1 mmol) in methanol (0.5 mL) and dichloromethane (10 mL) were successively layered benzene (3 mL) and a mixed solution of $AgCF_3SO_3$ (0.0257 g, 0.1 mmol) in benzene (5 mL) and acetonitrile (0.5 mL). The vial was covered in aluminum foil, and the solvents were allowed to diffuse slowly at room temperature. The orange prism crystals suitable for X-ray structure determination were formed several days later. Yield: 0.0291 g, 41%. IR (cm^{-1}): 3452 (s), 1687 (vs), 1660(m), 1610(m), 1548 (vs), 1490(s), 1420(m), 1334(m), 1301(s), 1275(s), 1237(s), 1166(m), 1022(s), 639(m). Anal. Calcd for $C_{23}H_{21}AgF_3FeN_4O_{6.5}S$: C, 38.93; H, 2.981; N, 7.889. Found: C, 38.90; H, 2.975; N, 7.894.

Synthesis of $[Ag_2(3\text{-BPFA})_2](CF_3CO_2)_2\cdot 2CH_3CN\cdot C_6H_6$ (5). Upon a solution of 3-BPFA (0.0426 g, 0.1 mmol) in methanol (0.5 mL) and dichloromethane (10 mL) were successively layered benzene (3 mL) and a mixed solution of $AgCF_3CO_2$ (0.0221 g, 0.1 mmol) in benzene (5 mL) and acetonitrile (1 mL). The vial was covered in aluminum foil, and the solvents were allowed to diffuse slowly at room temperature. The orange prism crystals suitable for X-ray structure determination were formed several days later. Yield: 0.0451 g, 62%. IR (cm^{-1}): 3301 (m), 1657 (vs), 1606(m), 1547 (vs), 1484(s), 1414(m), 1329(m), 1299(s), 1243(w), 1202(s), 1338(s), 1027(w), 827(m), 799(m), 720(m), 695(m). Anal. Calcd for $C_{29}H_{24}AgF_3FeN_5O_4$: C, 47.90; H, 3.326; N, 9.629. Found: C, 47.97; H, 3.330; N, 9.654.

Synthesis of $[Hg_2(3\text{-BPFA})_2Br_4]$ (6). To a solution of $HgBr_2$ (0.0180 g, 0.05 mmol) in methanol (10 mL) was slowly added 3-BPFA (0.0426 g, 0.1 mmol) in methanol (10 mL) at room temperature. The mixture was stirred at room temperature for 20 min in an aluminum-foil-covered 25 mL flask and filtered. The resulting mixture stood in the dark at room temperature. The orange block crystals suitable for X-ray structure determination were formed several weeks later. Yield: 0.0181 g, 46%. IR (cm^{-1}): 3321 (m), 1675(s), 1650 (vs), 1601(m), 1540 (vs), 1484(s), 1454(m), 1413(m), 1298(s), 1242(m), 802(m), 693(m). Anal. Calcd for $C_{44}H_{36}Br_4Fe_2Hg_2N_8O_4$: C, 33.59; H, 2.307; N, 7.122. Found: C, 33.89; H, 2.335; N, 7.187.

Synthesis of $[Zn(3\text{-BPFA})_2(SCN)_2]_n$ (7). To a solution of $Zn(SCN)_2$ (0.0091 g, 0.05 mmol) in methanol (5 mL) was slowly added 3-BPFA (0.0426 g, 0.1 mmol) in methanol (10 mL) at room temperature. The mixture was stirred at room temperature for 20 min in an aluminum-foil-covered 25 mL flask and filtered. The resulting mixture stood in the dark at room temperature. The orange bar crystals suitable for X-ray structure determination were formed several days later. Yield: 0.0300 g, 58%. IR (cm^{-1}): 3382 (m), 2052(vs), 1668(vs), 1648 (m), 1601(m), 1583(m), 1531 (vs), 1485(s), 1419(s), 1402(m), 1293(m), 1282(m), 802(m), 705(m). Anal. Calcd for $C_{46}H_{36}Fe_2N_{10}O_4S_2Zn$: C, 53.43; H, 3.511; N,13.55. Found: C, 52.58; H, 3.525; N, 13.03.

Synthesis of $[Zn(3\text{-BPFA})_2(N_3)_2]_n$ (8). To a solution of $Zn(ClO_4)_2\cdot 6H_2O$ (0.0188 g, 0.05 mmol) in methanol (10 mL) and NaN_3 (0.0065 g, 0.1 mmol) in water (0.5 mL) was slowly added 3-BPFA (0.0426 g, 0.1 mmol) in methanol (10 mL) at room temperature. The mixture was stirred at room temperature for 15 min in an aluminum-foil-covered 25 mL flask and filtered. The resulting mixture stood in the dark at room temperature. The orange bar crystals suitable for X-ray structure determination were formed several days later. Yield: 0.0210 g, 42%. IR (cm^{-1}): 3388 (s), 2049(vs), 1667(vs), 1648 (m), 1601(m), 1581(m), 1529 (vs), 1485(s), 1417(s), 1404(m), 1293(m), 1281(m), 801(m), 706(m). Anal. Calcd for $C_{44}H_{36}Fe_2N_{14}O_4Zn$: C, 52.75; H, 3.622; N, 19.57. Found: C, 52.61; H, 3.625; N, 19.43.

Synthesis of $[Cd(3\text{-BPFA})_2Br_2]_n$ (9). To a solution of $CdBr_2$ (0.0136 g, 0.05 mmol) in methanol (10 mL) was slowly added 3-BPFA (0.0426 g, 0.1 mmol) in methanol (10 mL) at room temperature. The mixture was stirred at room temperature for 15 min in an aluminum-foil-covered 25 mL flask and filtered. The resulting mixture stood in the dark at room temperature. The orange bar crystals suitable for X-ray structure determination were formed several weeks later. Yield: 0.0225 g, 40%. IR (cm^{-1}): 3385 (m), 1666(s), 1647 (s), 1599(m), 1532(vs), 1483(s), 1422(s), 1283(m), 800(m), 700(m). Anal. Calcd for $C_{44}H_{36}Br_2CdFe_2N_8O_4$: C, 46.99; H, 3.223; N, 9.958. Found: C, 46.83; H, 3.225; N, 9.965.

Table 1. Crystallographic Data for Complexes **4**−**7**

	4	5	6	7
CCDC	643825	643826	286348	273382
formula	$C_{23}H_{21}AgF_3FeN_4O_{6.5}S$	$C_{29}H_{24}AgF_3FeN_5O_4$	$C_{44}H_{36}Br_4Fe_2Hg_2N_8O_4$	$C_{46}H_{36}Fe_2N_{10}O_4S_2Zn$
formula weight	710.22	727.25	1573.33	1034.04
crystal system	monoclinic	triclinic	monoclinic	monoclinic
crystal size/mm^3	0.42 × 0.35 × 0.33	0.42 × 0.23 × 0.18	0.29 × 0.24 × 0.08	0.39 × 0.16 × 0.09
space group	$C2/c$	$P\bar{1}$	$P2(1)/c$	$P2(1)/c$
a/Å	25.378(17)	7.935(3)	19.1194(11)	14.0398(11)
b/Å	12.779(9)	13.767(5)	7.2281(4)	13.6443(11)
c/Å	19.657(13)	14.060(5)	17.8588(10)	10.5322(8)
α/deg	90.00	84.828(3)	90.00	90.00
β/deg	126.688(12)	75.688(3)	112.5040(10)	90.8180(10)
γ/deg	90.00	79.132(4)	90.00	90.00
V/Å^3	5112(6)	1459.9(9)	2280.1(2)	2017.4(3)
D_c/Mg m^{-3}	1.846	1.654	2.292	1.702
Z	8	2	2	2
F(000)	2840	730	1480	1056
μ/mm^{-1}	1.487	1.230	10.894	1.465
reflections collected	13470	6587	13628	10334
reflections unique	4498	4275	5199	3555
R(int)	0.0316	0.0180	0.0309	0.0217
data/restraints/params	4498/0/357	4275/0/389	5199/0/289	3555/0/303
final R indices[$I > 2\sigma(I)$]	R_1 = 0.0572	R_1 = 0.0473	R_1 = 0.0311	R_1 = 0.0277
	wR_2 = 0.1098	wR_2 = 0.1160	wR_2 = 0.0749	wR_2 = 0.0756
R indices(all data)	R_1 = 0.0667	R_1 = 0.0616	R_1 = 0.0425	R_1 = 0.0329
	wR_2 = 0.1143	wR_2 = 0.1259	wR_2 = 0.0891	wR_2 = 0.0890
GOF on F^2	1.049	1.018	1.030	1.023

Synthesis of $[Cd(3\text{-BPFA})_2(H_2O)_2]_n(NO_3)_{2n}$ (10). To a solution of $Cd(NO_3)_2 \cdot 4H_2O$ (0.0154 g, 0.05 mmol) in methanol (10 mL) was slowly added 3-BPFA (0.0426 g, 0.1 mmol) in methanol (10 mL) at room temperature. The mixture was stirred at room temperature for 20 min in an aluminum-foil-covered 25 mL flask and filtered. The resulting mixture stood in the dark at room temperature. Orange bar crystals suitable for X-ray structure determination were formed several weeks later. Yield: 0.0310 g, 55%. IR (cm^{-1}): 3401 (m), 3377(m), 1668(vs), 1648 (m), 1602 (m), 151(m), 1536(vs), 1485(s), 1429(s), 1383(s), 1329-(s), 1291(s), 802(m), 702(m). Anal. Calcd for $C_{44}H_{40}CdFe_2N_{10}O_{12}$: C, 46.98; H, 3.584; N, 12.45. Found: C, 46.76; H, 3.588; N, 12.18.

Synthesis of $[Hg(3\text{-BPFA})_2Cl_2]_n$ (11). To a solution of $HgCl_2$ (0.0136 g, 0.05 mmol) in methanol (10 mL) was slowly added 3-BPFA (0.0426 g, 0.1 mmol) in methanol (10 mL) at room temperature. The mixture was stirred at room temperature for 20 min in an aluminum-foil-covered 25 mL flask and filtered. The resulting mixture stood in the dark at room temperature. The orange block crystals suitable for X-ray structure determination were formed several days later. Yield: 0.0326 g, 58%. IR (cm^{-1}): 3402(m), 3383 (m), 1672(s), 1645 (s), 1599(m), 1532(vs), 1483(m), 1422(s), 1295(m), 1283(m), 800(m), 700(m). Anal. Calcd for $C_{44}H_{36}Cl_2Fe_2HgN_8O_4$: C, 47.02; H, 3.229; N, 9.97. Found: C, 47.02; H, 3.250; N, 10.11.

X-ray Crystallography. X-ray diffraction data were collected at 293(2) K on a Bruker-AXS SMART CCD area detector diffractometer using ω rotation scans with a scan width of 0.3° and Mo−K_α radiation (λ = 0.71073 Å). The structures were solved by direct methods and refined with full-matrix least-squares technique using SHELXTL.[17] Anisotropic thermal parameters were applied to all non hydrogen atoms. All of the hydrogen atoms in these structures are located from the differential electron density map and constrained to the ideal positions in the refinement procedure. The crystallographic calculations were conducted using the SHELXL-97 programs. Crystal data and experimental details for all crystals are given in Table 1 and 2.

(17) Sheldrick, G. M. *SHELXTL*, version 6.10; Bruker Analytical X-ray Systems: Madison, WI, 2001.

Results and Discussion

As indicated in Scheme 1, three typical conformations (I, II, and III) and various intermediates exist for 3-BPFA, which suggest this "building unit" is able to form a variety of polymeric patterns in self-assemblies. The synthetic strategy for operating the flexible "arms" is schematically depicted in Scheme 3. The ligand 3-BPFA reacts readily with a variety of ions, namely, Cu^{II}, Ni^{II}, Co^{II}, Ag^{I}, Zn^{II}, Cd^{II}, and Hg^{II}, to construct different assemblies. Four types of basic motifs can be constructed from the 3-BPFA module, in which the two Cp-"arm" units of 3-BPFA can form different arrangements around the metal ion: type I, helix; type II, cage or capsule; type III, dimer or macrocycle; type IV, M′-MOFs. Obviously, the shapes of the architectures are determined by the angle between two arms in 3-BPFA, which results from the flexibility of two Cp-CO-aminopyridine units in the ligand 3-BPFA. Besides the angle of ligand, the metal connection mode is another key tectonic factor for the self-assembly. Herein we have structurally characterized the type I a helical chain for free ligand 3-BPFA by intermolecular N−H···O=C hydrogen bonds, type II a coordination cage for Cu^{II} complex and two coordination capsules for Co^{II} and Ni^{II} complexes, type III two dimers for Ag^{I} complexes and a coordination macrocycle for Hg^{II} complex, type IV five heterometallic MOFs for Zn^{II}, Cd^{II}, and Hg^{II} complexes.

These complexes do not dissolve in common solvents, such as acetone, chloroform, ethanol, methylene chloride, tetrahydrofuran, they only slightly dissolve in methanol, and they easily dissolve in highly polar solvents such as DMF. All these compounds are air stable for a long time, and their structures are detailedly described below.

Helical Supramolecular Structure of 3-BPFA. To compare the conformation change of 3-BPFA in the supramolecular architectures, the structure of the free ligand was determined. As shown in Figure 1, there are two weak C−H···O hydrogen bonding interactions in 3-BPFA, with the distances 2.243 Å for H(8)···O(1), and 2.260 Å for H(22)···O(2), respectively, which achieves a pair of

Table 2. Crystallographic Data for Complexes **8**−**11**

	8	**9**	**10**	**11**
CCDC	286347	273383	294230	273384
formula	$C_{44}H_{36}Fe_2N_{14}O_4Zn$	$C_{44}H_{36}Br_2CdFe_2N_8O_4$	$C_{44}H_{40}CdFe_2N_{10}O_{12}$	$C_{44}H_{36}Cl_2Fe_2HgN_8O_4$
Formula weight	1001.94	1124.73	1124.97	1124.00
crystal system	monoclinic	monoclinic	monoclinic	monoclinic
crystal size/mm^3	0.20 × 0.16 × 0.15	0.30 × 0.20 × 0.14	0.16 × 0.06 × 0.06	0.60 × 0.40 × 0.35
space group	*P*2(1)/*c*	*P*2(1)/*c*	*P*2(1)/*c*	*P*2(1)/*c*
a/Å	13.3576(15)	13.9008(14)	14.6740(11)	13.6585(13)
b/Å	13.7387(16)	13.6615(14)	13.4989(10)	13.7182(13)
c/Å	10.5483(12)	10.6017(11)	10.4686(8)	10.6540(10)
α/deg	90.00	90.00	90.00	90.00
β/deg	90.00	90.593(2)	91.278(2)	91.114(2)
γ/deg	90.00	90.00	90.00	90.00
V/Å^3	1935.8(4)	2013.2(4)	2073.1(3)	1995.9(3)
D_c/Mg m^{-3}	1.719	1.855	1.796	1.870
Z	2	2	2	2
F(000)	1024	1116	1132	1108
μ/mm^{-1}	1.423	3.276	1.281	4.745
reflections collected	10997	12163	9973	12225
reflections unique	4411	4510	3648	4543
R(int)	0.0516	0.0344	0.0384	0.0248
data/restraints/params	4411/0/295	4510/0/277	3648/0/313	4543/0/ 349
final *R* indices[$I > 2\sigma(I)$]	R_1 = 0.0346	R_1 = 0.0553	R_1 = 0.0585	R_1 = 0.0247
	wR_2 = 0.0701	wR_2 = 0.1377	wR_2 = 0.1320	wR_2 = 0.0623
R indices(all data)	R_1 = 0.0505	R_1 = 0.0665	R_1 = 0.0670	R_1 = 0.0282
	wR_2 = 0.0995	wR_2 = 0.1444	wR_2 = 0.1415	wR_2 = 0.0689
GOF on F^2	1.025	1.016	1.056	1.021

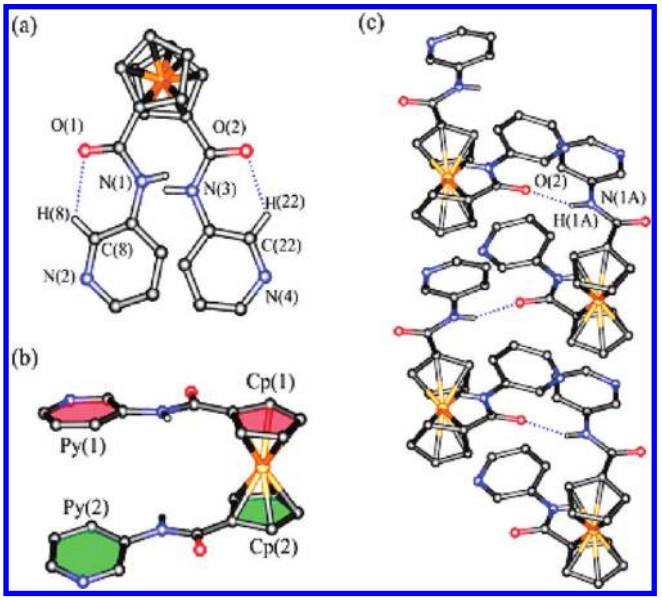

Figure 1. (a) View (top) of 3-BPFA showing the *trans*-configuration of two intramolecular C−H···O hydrogen bonds; (b) The view (side) of 3-BPFA exposing the nonplanar characteristic between pyridyl rings and related Cp planes; (c) Helical structure of 3-BPFA by hydrogen bonds along the *b* axis. Partial H atoms were omitted for clarity in this and the following figures.

six-membered steady structure. These intramolecular H-bonding interactions also consist in complexes **1**−**11**, although they exhibit different modes (see Supporting Information). Additionally, both pyridyl rings of the ligand are not coplanar with the linked Cp planes, with the twist angles of 11.83° and 10.96°, respectively (Figure 1b). Although such twist is also observed in complexes **1**−**11**, the corresponding dihedral angles between the pyridyl rings and Cp planes have great variations among these complexes (Supporting Information, Table S1).

3-BPFA crystals pack into supramolecular helices via strong intermolecular hydrogen bonding interactions (H(1A)···O(2) 2.14 Å, N(1)−H(1A)···O(2) 160.2°) that extend indefinitely through the crystal lattice (Figure 1c). Two pyridyl groups exhibit a *trans*-configuration in 3-BPFA owing to these hydrogen bonding interactions, which is a typical conformation of mode I (Scheme 1). It has been proven that ferrocene can act as a molecular scaffold to support *β*-sheet-like interactions between two peptide chains via H-bonding between amide groups.[18] It was suggested that this H-bonding information is helpful to study mechanism of protein folding or biochemical processes, and to generate novel biological materials and "soft" materials.[19]

Generally, the properties of "soft" materials result from the characterizations of the macromolecules, in particular the entanglements that arise when a large number of repeating monomers are linked into a long chain. Obviously, the central properties of such materials are from noncovalent interactions, which have a rapid response to the environment change. Furthermore, the strength and selectivity of noncovalent interactions can be adjusted by synthetic conditions. Thus, the synthesis of polymers by linking monomers via noncovalent interactions (vide post complexes **1**−**6**), or the assembling of polymer networks through noncovalent interactions (vide post complexes **7**−**11**), would represent an attractive approach to the construction of "soft" materials.

(18) (a) Chowdhury, S.; Schatte, G.; Kraatz, H.-B. *Angew. Chem., Int. Ed.* **2008**, *47*, 7056–7059. (b) Chowdhury, S.; Schatte, G.; Kraatz, H.-B. *Angew. Chem., Int. Ed.* **2006**, *45*, 6882–6884. (c) Kirin, S. I.; Kraatz, H.-B.; Metzler-Nolte, N. *Chem. Soc. Rev.* **2006**, *35*, 348–354. (d) Chowdhury, S.; Schatte, G.; Kraatz, H.-B. *Angew. Chem.* **2006**, *45*, 6882–6884.

(19) (a) Osterhout, J. J. *Protein Pept. Lett.* **2005**, *12*, 159–164. (b) Sadowsky, J. D.; Schmit, M. A.; Lee, H. S.; Umezawa, S. M.; Wang, N.; Tomita, Y.; Gellman, S. H. *J. Am. Chem. Soc.* **2005**, *127*, 11966–11968. (c) Balzani, V.; Credi, A.; Raymo, F. M.; Stoddart, J. F. *Angew. Chem., Int. Ed.* **2000**, *39*, 3348–3391. (d) Hecht, S. *Mater. Today* **2005**, *8*, 48–55.

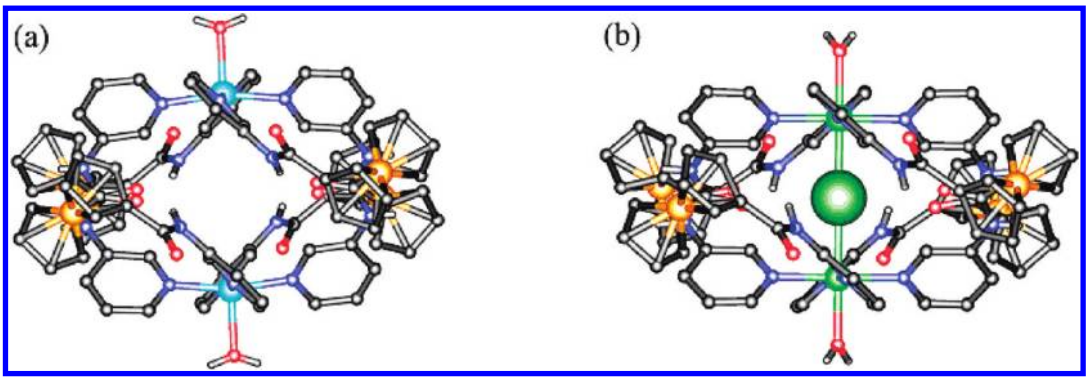

Figure 2. (a) Single-crystal X-ray structure of the $[(3\text{-BPFA})_4Cu_2(H_2O)_2]^{4+}$ cage; (b) Side view of single-crystal X-ray structure of the $[(3\text{-BPFA})_4M_2(\mu\text{-Cl})(H_2O)_2]^{3+}$ capsules. (M = Ni(II) for **2**; M = Co(II) for **3**). ClO_4^- anions and partial solvent molecules are omitted for clarity.

Coordination Cage and Molecular Pseudo-Capsules. In all of the three cage-type coordination structures, the 3-BPFA molecules were linked by the second metal ions and resulted in bimetallic complexes with stoichiometry of $M_2(3\text{-BPFA})_4$ (M = Cu, Ni, and Co for **1**, **2**, and **3**, respectively), as shown in Figure 2. (See detailed earlier report)[13] In complexes **1**−**3**, the bridging molecule 3-BPFA exhibits similar conformation to bond two metal centers, in which two Cp-"arm" units reversely rotate about 72°. This confirmation is induced by strong coordinative interactions of 3-BPFA to the second metal ions, which results in a "head-to-head" conformation of N_{Py} atoms between two "arms" of 3-BPFA (Scheme 1: type III). It is difficult that the cage-type structure is assembled through the use of 4-position derivations of pyridine, which are easy to form macrocyclic assemblies, such as 1,1′-bis[(4-pyridylamino)carbonyl]ferrocene[20,9a], 1,1′-bis[(4-pyridylamino)carbonyl]cobaltocene,[21], 1,1′-bis-(4-pridyl)ferrocene[5c], and 1,1′-bis(4-pridyl-ethynyl)ferrocene.[7a,22] On this aspect, 3-position derivations of pyridine have an advantage for the construction of molecular spheres.[23]

All three compounds were prepared under the same conditions including solvent system, metal-to-ligand ratio, and temperature. The different structures of the three complexes indicate that the coordination properties of metals are crucial in determining the cage-type structure of complexes **1**−**3**. The cavity of **1** is owed to the preference of penta-coordination geometry for Cu^{II}.[24] Whereas for **2** and **3**, the "encapsulated" Cl^- anion is an essential for six coordination geometries of Ni^{II} and Co^{II}.

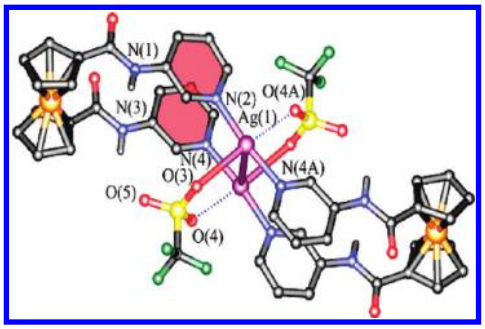

Figure 3. Self-assembled dimeric unit of 3-BPFA and $AgCF_3SO_3$ in complex **4**. The solvent molecules are omitted for clarity.

Dimers and Coordination Macrocycle. It is well-known that the "soft" Ag(I) ion, with a d^{10} electronic configuration, has a strong tendency to display various coordination geometries.[25] Thus, the Ag(I) ion readily accommodates the geometry variation induced by various ligands and is suitable to form novel structures.

Upon slow diffusion of a mixed solution of $AgCF_3SO_3$ in benzene and acetonitrile into a solution of 3-BPFA in dichloromethane, the orange single crystals of $[Ag_2(3\text{-BPFA})_2](CF_3SO_3)_2\cdot 3H_2O$ (**4**) were obtained. Single-crystal X-ray analysis reveals, as shown in Figure 3, a discrete dimer formed from two crystallographically equivalent silver(I) centers. Each Ag(1) center is coordinated by two nitrogen atoms from two different 3-BPFA ligands, with an almost linear angle of 172.86°. Both Ag(1)−N(2) and Ag(1)−N(4) bond distances are 2.125(5) Å. Two silver centers bind to two $CF_3SO_3^-$ anions, which are located on different sides of the dimer through anion coordination interactions with Ag−O bonds length of 2.86 Å and 3.20 Å, respectively. Only a slight deviation from a linear O−Ag−O arrangement is observed (164.85°). As a result, two silver atoms are wrapped up by four different supported ligands to form a gear-wheel-like structure with the Fe···Fe distance of 16.97 Å. The bond distance (3.22 Å) of the Ag−Ag pair, which forms the axis of dimer gear structure, is distinctly shorter than the sum of van der Waals radii of two silver atoms (3.44 Å).[26] This distance is significantly shorter than the Ag−Ag distances reported previously in the dimetallic complexes supported by ferrocene-based ligands (ranging from 3.50 to 3.79 Å).[5c,7a] The heteroatom distances (Ag···Fe) are 8.33 Å and 8.94

(20) Moriuchi, T.; Ikeda, I.; Hirao, T. *Organometallics* **1995**, *14*, 3578–3580.
(21) Braga, D.; Polito, M. *Cryst. Growth Des.* **2004**, *4*, 769–774.
(22) Lindner, E.; Zong, R. F.; Eichele, K. *Phosphorous, Sulfur Silicon* **2001**, *169*, 219–222.
(23) (a) Fan, J.; Zhu, H.-F.; Okamura, T.; Sun, W.-Y.; Tang, W.-X.; Ueyama, N. *Chem.—Eur. J.* **2003**, *91*, 4724–4731. (b) Hiraoka, S.; Harano, K.; Shiro, M.; Ozawa, Y.; Tasuda, N.; Toriumi, K.; Shionoya, M. *Angew. Chem., Int. Ed.* **2006**, *45*, 6488–6491. (c) Mukherjee, P. S.; Das, N.; Stang, P. J. *J. Org. Chem.* **2004**, *69*, 3526–3529.
(24) (a) Sunatsuki, Y.; Motoda, Y.; Matsumoto, N. *Coord. Chem. Rev.* **2002**, *226*, 199–209. (b) Lu, J. Y. *Coord. Chem. Rev.* **2003**, *246*, 327–347.
(25) (a) Wei, K.-J.; Xie, Y.-S.; Ni, J.; Zhang, M.; Liu, Q.-L. *Inorg. Chem. Commun.* **2006**, *9*, 926–930. (b) Wei, K.-J.; Ni, J.; Gao, J.; Liu, Y.; Liu, Q.-L. *Eur. J. Inorg. Chem.* **2007**, 3868–3880. (c) Dong, Y.-B.; Ma, J.-P.; Huang, R.-Q.; Smith, M. D.; zur Loye, H.-C. *Inorg. Chem.* **2003**, *42*, 294–300. (d) Dong, Y.-B.; Cheng, J.-Y.; Huang, R.-Q.; Smith, M. D.; zur Loye, H.-C. *Inorg. Chem.* **2003**, *42*, 5699–5706. (e) Dong, Y.-B.; Geng, Y.; Ma, J.-P.; Huang, R.-Q. *Organometallics* **2006**, *25*, 447–462.
(26) Bondi, A. *J. Phys. Chem.* **1964**, *68*, 441–451.

Å, respectively, which are slightly longer than those in **1**−**3** (ranging from 7.72 to 8.34 Å) owing to the twisted effect between two Cp-"arm" groups of 3-BPFA in complexes **1**−**3**.

Both theoretical and experimental studies have demonstrated that argentophilic and $\pi\cdots\pi$ interactions can be both "cooperative" and "competitive" in the same supramolecular motif, which highly depend on interplanar distance of two arene moieties.[27] Generally, the "cooperative" interactions occur when this interplanar distance is longer than the equilibrium distance, which is the interplanar distance reaching the energy minimum of the supramolecular system. On the other hand, pyridyl units of 3-BPFA become easily polarized by the presence of metal coordination. In other words, two parallel conformations can exist in 3-BPFA complexes: head-to-tail and head-to-head (Supporting Information, Scheme S1). The head-to-tail alignment is usually formed when such conformation is energetically more favorable,[28] which typically occurs if the aromatic fragments are supported by additional interactions, such as covalent bonds, coordination bonds, or metal−metal interactions.[29] The less common head-to-head alignment is present in complex **4** with intramolecular $\pi\cdots\pi$ stacking interactions between two pyridyl-rings (centroid-to-centroid distance 3.50 Å, 6.95° tilte). Therefore, the Ag−Ag interaction is probably supported by these $\pi\cdots\pi$ interactions in **4**. Similar interactions have been observed in a few complexes.[27−29] Obviously, these two dominant intramolecular interactions, metallophilicity and $\pi\cdots\pi$ stacking, facilitate the close packing of the dimer configuration in **4**.

These discrete units are linked via cation-π (or Ag-Cp) interactions to build 2D frameworks. As shown in Figure 4, each Ag^{I} ion is locked on the top of the Cp ring of the neighboring ferrocene moiety through weak $Ag^{I}\cdots\pi$ interactions. The Ag^{I} ions sit nearly above the center of the Cp rings. The $Ag^{I}\cdots C$ distance ranges from 3.215 to 3.603 Å, which indicates the interaction is fairly weak.[30] As a result, the Cp ring coordinates to the silver atom in the neighbor molecule and results in a rare bimetallic sandwich-of-sandwich structure (Figure 4b). Furthermore, guest water molecules are locked in host-networks via multiple hydrogen bonding interactions. (see Supporting Information) In addition to filling the void spaces in the MOFs, the presence of guest water molecules can also contribute to the packing of the complex and enhance the stability of MOFs.

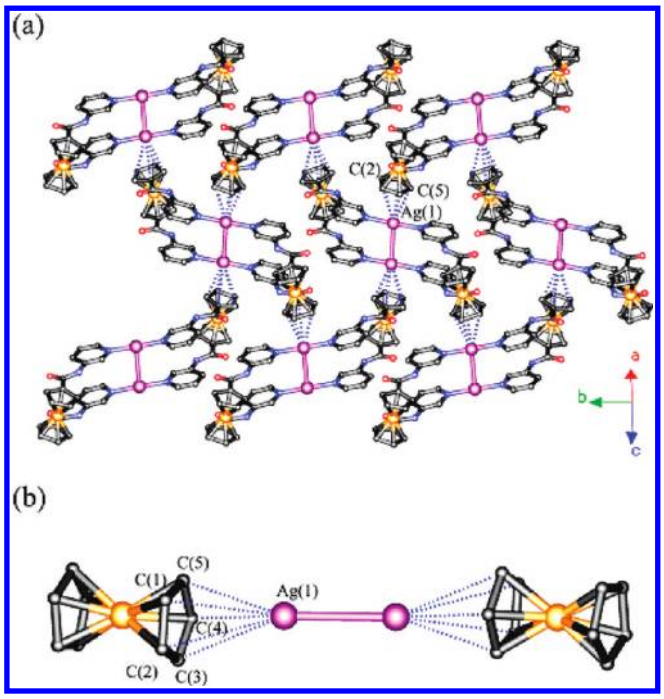

Figure 4. (a) 2D supramolecular networks formed via Ag$\cdots\pi$ interactions in **4**; (b) the structure of sandwich-of-sandwich in **4** (C(4)−Ag(1) 3.242 Å; C(3)−Ag(1) 3.512 Å; C(2)−Ag(1) 3.603 Å; C(1)−Ag(1) 3.424 Å; C(5)−Ag(1) 3.215 Å). The solvent molecules and counterions are omitted for clarity.

Besides coordination bonding, various interactions have been applied to construct periodic networks, including covalent bonding,[31] hydrogen bonding,[5d,25a,32] $\pi\cdots\pi$ stacking,[5f,25b] ionic interactions,[33] lipophilic interactions,[34] metal−metal interactions,[28,35] and halogen bonding.[36] The structure of **4** provides an outstanding example of cation-π interactions in the construction of periodic networks. This cation-π interaction is proven to play a critical role in numerous biological recognition processes,[37] but it has received very little attention in the

(27) (a) Burini, A.; Fackler, J. P., Jr.; Galassi, R.; Grant, T. A.; Omary, M. A.; Rawashdeh-Omary, M. A.; Pietroni, B. R.; Staples, R. J. *J. Am. Chem. Soc.* **2000**, *122*, 11264–11265. (b) Rawashdeh-Omary, M. A.; Omary, M. A.; Fackler, J. P., Jr. *J. Am. Chem. Soc.* **2001**, *123*, 9689–9691. (c) Yang, G.; Raptis, R. G. *Inorg. Chem.* **2003**, *42*, 261–263. (d) Olmstead, M. M.; Jiang, F.-L.; Attar, S.; Balch, A. L. *J. Am. Chem. Soc.* **2001**, *123*, 3260–3267. (e) Hayashi, A.; Olmstead, M. M.; Attar, S.; Balch, A. L. *J. Am. Chem. Soc.* **2002**, *124*, 5791–5795. (f) Puddephatt, R. J. *Chem. Commun.* **1998**, 1055–1062. (g) Hao, L.-J.; Lachicotte, R. J.; Gysling, H. J.; Eisenberg, R. *Inorg. Chem.* **1999**, *38*, 4616–4617.

(28) Zhang, J.-P.; Wang, Y.-B.; Huang, X.-C.; Lin, Y.-Y.; Chen, X.-M. *Chem.—Eur. J.* **2005**, *11*, 552–561.

(29) (a) Janiak, C. *J. Chem. Soc., Dalton Trans.* **2000**, 3885. (b) Khlobystov, A. N.; Blake, A. J.; Champness, N. R.; Lemenovskii, D. A.; Majouga, A. G.; Zyk, N. V.; Schröer, M. *Coord. Chem. Rev.* **2001**, *222*, 155−192 and refs cited therein.

(30) (a) Dong, Y.-B.; Zhang, Q.; Wang, L.; Ma, J.-P.; Huang, R.-Q.; Shen, D.-Z.; Chen, D.-Z. *Inorg. Chem.* **2005**, *44*, 6591–6593. (b) Dong, Y.-B.; Geng, Y.; Ma, J.-P.; Huang, R.-Q. *Inorg. Chem.* **2005**, *44*, 1693–1703. (c) Dong, Y.-B.; Wang, P.; Huang, R.-Q.; Smith, M. D. *Inorg. Chem.* **2004**, *43*, 4727–4739. (d) Dong, Y.-B.; Geng, Y.; Ma, J.-P.; Huang, R.-Q. *Organometallics.* **2006**, *25*, 447–462. (e) Wang, P.; Dong, Y.-B.; Ma, J.-P.; Huang, R.-Q.; Smith, M. D. *Cryst. Growth Des.* **2005**, *5*, 701–706. (f) Dong, Y.-B.; Jin, G.-X.; Zhao, X.; Tang, B.; Huang, R.-Q.; Smith, M. D.; Stitzer, K. E.; zur Loye, H.-C. *Organometallics.* **2004**, *23*, 1604–1609. (g) Munakata, M.; Wu, L. P.; Ning, G. L. *Coord. Chem. Rev.* **2000**, *198*, 171–203. (h) Ning, G. L.; Wu, L. P.; Sugimoto, K.; Munakata, M.; Kuroda-Sowa, T.; Mackawa, M. *J. Chem. Soc., Dalton Trans.* **1999**, 2529–2536. (i) Zheng, S.-L.; Tong, M.-L.; Tan, S.-D.; Wang, Y.; Shi, J.-X.; Tong, Y.-X.; Lee, H. K.; Chen, X.-M. *Organometallics.* **2001**, *20*, 5319–5325.

(31) Oku, T.; Furusho, Y.; Takata, T. *Angew. Chem., Int. Ed.* **2004**, *43*, 966–969.

(32) Hosseini, M. W. *Acc. Chem. Res.* **2005**, *38*, 313–323.

(33) Ballabh, A.; Trivedi, D. R.; Dastidar, P. *Cryst. Growth Des.* **2005**, *5*, 1545–1553.

(34) Madalan, A. M.; Kravtsov, V. C.; Simonov, Y. A.; Voronkova, V.; Korobchenko, L.; Avarvari, N.; Andruh, M. *Cryst. Growth Des.* **2005**, *5*, 45–47.

(35) Khlobystov, A. N.; Blake, A. J.; Champness, N. R.; Lemenovskii, D. A.; Majouga, A. G.; Zyk, N. V.; Schröder, M. *Coord. Chem. Rev.* **2001**, *222*, 155–192.

(36) Metrangolo, P.; Resnati, G. *Chem.—Eur. J.* **2001**, *7*, 2511–2519.

(37) (a) Zacharias, N.; Dougherty, D. A. *Trends Pharmacol. Sci.* **2002**, *23*, 281–287. (b) Zhong, W.; Gallivan, J. P.; Zhang, Y.; Li, L.; Lester, H. A.; Dougherty, D. A. *Proc. Natl. Acad. Sci. U.S.A.* **1998**, *95*, 12088–12093. (c) Doyle, D. A.; Cabral, J. M.; Pfuetzner, R. A.; Kuo, A.; Gulbis, J. M.; Cohen, S. L.; Chait, B. T.; MacKinnon, R. *Science* **1998**, *280*, 69–77. (d) Gallivan, J. P.; Dougherty, D. A. *Proc. Natl. Acad. Sci. U.S.A.* **1999**, *96*, 9459–9464. (e) Kumpf, R. A.; Dougherty, D. A. *Science* **1993**, *261*, 1708–1710.

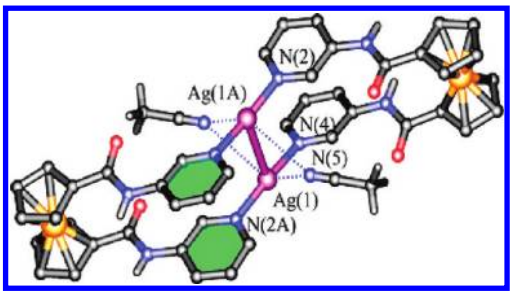

Figure 5. Self-assembled dimeric unit of 3-BPFA and $AgCF_3CO_2$ in **5**. The benzene molecules and anions are omitted for clarity.

assembly of extended networks.[38] The observation in this work shows that ferrocene can be a good candidate for creating extended networks through cation-π interactions.

To investigate the effect of the counteranion on the construction of the 3-BPFA-Ag^I coordination dimer, the strong coordination anion $CF_3CO_2^-$ is used instead of the weak coordination anion $SO_3CF_3^-$. Orange crystals of $[Ag_2(3\text{-BPFA})_2](CF_3CO_2)_2 \cdot 2CH_3CN \cdot C_6H_6$ (**5**) were obtained using a similar method to that for complex **4**. Single-crystal X-ray analysis reveals that the complex **5** has a similar coordination core to the complex **4**, in which the dimer structure is constructed by a silver−silver center coordinated by two 3-BPFA in head-to-head mode (Figure 5). This observation suggests that the nature of silver ion is dominant in this dimeric assembly. It is characterized by the contact between the silver atoms such that the Ag−Ag vector is near-perpendicular to the nearly linear N(2A)−Ag(1)−N(4) vector (173.95°), in which the two angles are 87.87(11)° and 98.06(11)°, respectively. The two Ag−N bonds (2.155 and 2.150 Å) are slightly longer than those in **4**, while the Ag−Ag distance (3.19 Å) is slightly shorter than that in **4**. The Fe···Fe distance (16.83 Å) and heteroatom distances (Ag···Fe) (8.52 Å and 8.61 Å) are similar to those in **4**.

Different from the anion coordination in **4**, two guest acetonitrile molecules in **5** are located on both sides of the molecular "wall" via weak Ag−N coordination interactions, in which the bond lengths of Ag(1)−N(5) and Ag(1A)−N(5) are 2.930 and 3.199 Å, respectively. The face-to-face $\pi\cdots\pi$ interactions featuring head-to-head alignments are formed in **5** as well, in which the pyridyl fragments are supported by metal−metal interactions. The centroid-to-centroid distance between two pyridyl rings is 3.63 Å and the corresponding dihedral angle is 14.66°, which is larger than that of **4**, indicating weaker $\pi\cdots\pi$ interactions than those in **4**. The weaker $\pi\cdots\pi$ interactions in **5** are probably due to the attractions of multiple H-bonds resulting from $CF_3CO_2^-$ anions and pyridyl rings (see Supporting Information). As a result, two pyridyl rings occur to the slightly offset conformation.

Although the bridging 3-BPFA units in **4** and **5** coordinate Ag^I centers in a similar "*cis*-" conformation to form dimers (type II motif in Scheme 1), the two "arms"

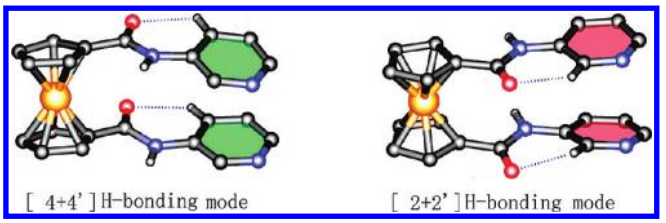

Figure 6. [4 + 4′] and [2 + 2′] intramolecular C−H···O hydrogen bonding modes of 3-BPFA in **4** and **5**, respectively.

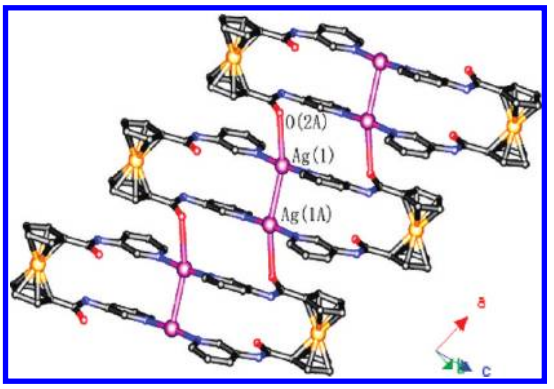

Figure 7. One-dimensional ladder-like structure of complex **5**.

of 3-BPFA adopt different configurations in two complexes, in which the orientation of pyridyl rings are in opposite direction. Relative to the amide groups, the pyridyl nitrogen atoms in complex **5** are *cis*- to carbonyl, which undergo ~180° rotation compared with the structure in **4**. In complex **4**, two C−H···O hydrogen-bonding interactions exhibit [4 + 4′] mode, while those introduce [2 + 2′] format in complex **5** (Figure 6). The result is likely to result from the supramolecular "steric hindrance effect" of $CF_3CO_2^-$ anions in **5**, which are locked on one side of Cp-"arm" groups by special triplex hydrogen bonding interactions (Supporting Information, Figure S8). That is, the anion is what directly drives the rotation of pyridyl rings around the C−N single bond.

The most interesting feature of complex **5** is that the coordination dimers are arranged in a linear formation and generate a ladder-like chain extended along the *a* axis (Figure 7). This structure is stabilized by Ag−O (2.909 Å) coordination from the silver atom in one dimer to the amide oxygen atom in the adjacent unit. The Ag−O coordination between dimer units constructs a one-dimensional chain, in which the nearest intrapolymer Ag···Ag distance between two adjacent dimers is 5.54 Å. This one-dimensional chain is further linked into a 2D network via C−H···O hydrogen-bonding between host-intrapolymer and guest-benzene molecule (Supporting Information, Figure S9).

Although the short intradimer metal−metal contacts in the two complexes (**4** and **5**) are formed by ligand bridging effects, the interdimer geometries for the polymer-of-dimers are different. Crystal packing effects can contribute to the ligand-supported metallophilicity found in individual crystal structures. However, the structural change should not only result from such weak forces, since the packing patterns for **4** and **5** are rather different. Additionally, the two Ag^I ions in **4** and **5** are held, which provide two rare examples suitable for studying metallophilic

(38) (a) Haneline, M. R.; GabbaW, F. P. *Angew. Chem., Int. Ed.* **2004**, *43*, 5471–5474. (b) Scholz, S.; Green, J. C.; Lerner, H.-W.; Bolte, M.; Wagner, M. *Chem. Commun.* **2002**, 36–37. (c) Morris, J. J.; Noll, B. C.; Honeyman, G.; O'Hara, C. T.; Kennedy, A. R.; Mulvey, R. E.; Henderson, K. W. *Chem.—Eur. J.* **2007**, *13*, 4418–4432.

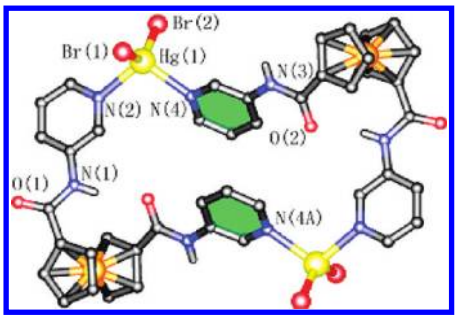

Figure 8. Self-assembled Fe/Hg metallamacrocycle of 3-BPFA and $HgBr_2$ in **6**.

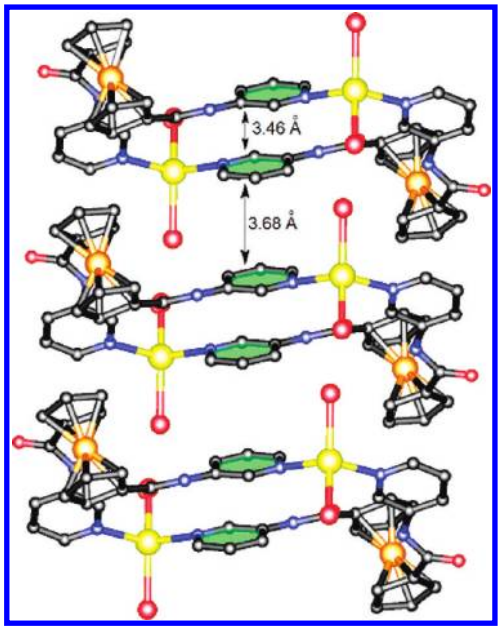

Figure 9. One-dimensional chain structure of complex **6** constructed via intra- and intermolecular face-to-face $\pi\cdots\pi$ stacking interactions.

attractions with the ligand supported in closed shell Ag^I systems.

Orange block crystals of $[Hg_2(3\text{-BPFA})_2Br_4]$ (**6**) were obtained from methanol solution of 3-BPFA and $HgBr_2$. Single crystal X-ray analysis reveals the macrocycle structure of this self-assembled complex (Figure 8). The tetranuclear macrocycle is composed of two 3-BPFA molecules bridged by two $[HgBr_2]$ units. The coordination geometry around the Hg^{II} center is a tetrahedral conformation with a N_2Br_2-donor environment (Hg−N(2) 2.380(4), Hg−N(4) 2.362(4), Hg−Br(1) 2.4868(7), Hg−Br(2) 2.5054(7) Å). Compared with complexes **4** and **5**, two Cp-"arm" groups are severely twisted in the Hg^{II} coordinated complex, although two pyridyl rings still adopt a "*cis*-" configuration in a distorted rectangle. Four metal atoms lie in a plane, and the Fe···Fe and Hg···Hg distances are 14.11 and 10.60 Å, respectively. The heteroatom distances (Hg···Fe) are 8.58 and 9.06 Å, respectively. The two N(4) pyridyl rings from two different 3-BPFA molecules on the macrocycle of both sides are oriented exactly parallel with the distance of 3.46 Å (Figure 9).

A detailed inspection of **6** reveals that the assembly is also held together by two intramolecular N−H···O hydrogen bonds (O···H 2.159 Å, ∠N−H···O 153.78°),

Scheme 4. Macrocyclic Building Unit $[M_4(syn\text{-}3\text{-BPFA})_2(anti\text{-}3\text{-BPFA})_2]$ in the Two Dimensional Mixed-MOFs[a]

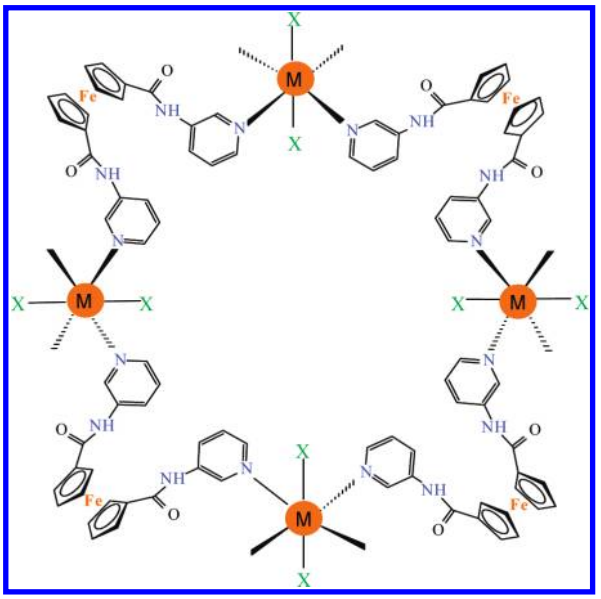

[a] M = Zn(II), X = SCN^- (**7**), N_3^-(**8**); M = Cd(II), X = Br^- (**9**); M = Cd(II), X = H_2O (**10**); M = Hg(II), X = Cl^- (**11**).

similar to those in complexes **1**−**3**. Two pyridyle nitrogen atoms in 3-BPFA in complex **6** adopt the same coordination conformation (type II in Scheme 1). Different from complexes **4** and **5**, two intramolecular parallel pyridyl rings favor a head-to-tail alignment with slightly offset conformation in **6**. This type of alignment also extends intermacrocycles, which forms a one-dimensional supramolecular chain via face-to-face $\pi\cdots\pi$ stacking interactions with the interplanar distance of 3.68 Å, as shown in Figure 9.

The existence and structural importance of $\pi\cdots\pi$ interactions are also well established, and they are observed in many complexes.[25b,28,39] The same as for the hydrogen bonding interaction, this π stacking interaction, as an important member of noncovalent interaction family, also contributes significantly to the alignment of the supramolecular structures in the crystalline state.

Heterometallic Metal-Organic Frameworks (M′-MOFs). The Zn^{II}, Cd^{II}, and Hg^{II} ions, with d^{10} electronic configurations, have demonstrated high binding affinity toward nitrogen donor ligands in a considerably large number of complexes.[39,40] The reaction of 3-BPFA with these three metal salts containing different anions generated five heterobimetallic MOFs: $[Zn(3\text{-BPFA})_2(SCN)_2]_n$ (**7**), $[Zn(3\text{-BPFA})_2(N_3)_2]_n$ (**8**), $[Cd(3\text{-BPFA})_2Br_2]_n$ (**9**), $[Cd(3\text{-BPFA})_2(H_2O)_2]_n(NO_3)_{2n}$ (**10**), and $[Hg(3\text{-BPFA})_2Cl_2]_n$ (**11**). In these assembled complexes, each M^{II} ion has a hexacoordination environment to accomplish an octahedral geometry around the metal center. Two pyridyle nitrogen atoms in two arms of 3-BPFA coordinate to two metal ions, and each metal ion binds to four pyridine N atoms from four different 3-BPFA ligands, which results in a series of

(39) (a) Wei, K.-J.; Xie, Y.-S.; Ni, J.; Zhang, M.; Liu, Q.-L. *Cryst. Growth Des.* **2006**, *6*, 1341–1350. (b) Sun, C.-Y.; Goforth, A. M.; Smith, M. D.; zur Loye, H.-C. *Inorg. Chem.* **2003**, *42*, 5685–5692. (c) Wu, G.; Wang, X.-F.; Okamura, T.; Sun, W.-Y.; Ueyama, N. *Inorg. Chem.* **2006**, *45*, 8523–8532.

(40) (a) Das, S.; Hung, C.-H.; Goswami, S. *Inorg. Chem.* **2003**, *42*, 8592–8597. (b) Fleischer, H.; Hardt, S.; Schollmeyer, D. *Inorg. Chem.* **2006**, *45*, 8318–8325.

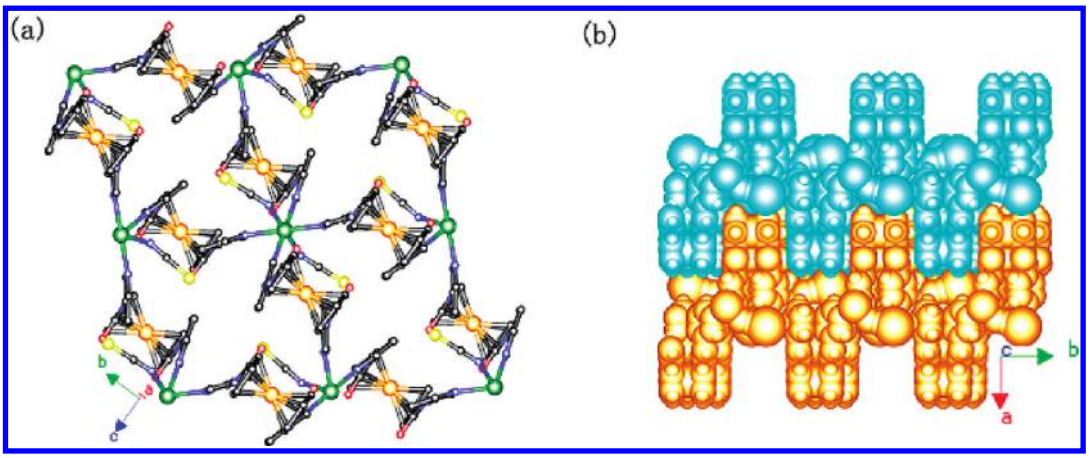

Figure 10. (a) View of 2D network of complex **7**; (b) two adjacent layers interact with each other through weak C−H···S interactions, giving an ···*AAA*··· packing sequence of 2D M′-MOFs in the crystal lattice.

Table 3. Selected Geometric Parameters [Å and deg] of Eight Metal Units in Complexes **7**−**11**

complex	adjacent M···M distances	adjacent Fe···Fe distances		acute angle M···M···M
7	8.618	5.498	17.391	75.33
8	8.661	5.510	17.319	75.03
9	8.646	5.541	17.608	75.62
10	8.541	5.486	17.699	75.59
11	8.635	5.585	17.753	75.67

2D MOFs. Two counteranions coordinate to M^{II} center on different sides of frameworks. Distinctively, instead of the anion coordination in **7**−**9**, two water molecules coordinate to the cadmium center in complex **10**. In these five MOFs, the basic building unit is the similar octa-metal macrocyclic structure [M_4(*syn*-3-BPFA)$_2$(*anti*-3-BPFA)$_2$]. As shown in Scheme 4, four M^{II} ions are coplanar in the macrocyclic unit. Relative to the $M^{II}{}_4$ plane, two adjacent 3-BPFA ligands link two M^{II} ions in same *syn*-conformation, while the other two ligands bond two M^{II} centers in *anti*-conformation. As a result, a wave-type sheet is formed via the interlaced connection of *syn*- and *anti*-fashion structures.

Figure 10 shows the crystal structure of Zn−Fe M′-MOFs **7**, in which the macrocyclic structure is constituted by the repeating units of [Zn_4(*syn*-3-BPFA)$_2$(*anti*-3-BPFA)$_2$]. The four Zn^{II} ions are arranged in a rhombus shape through four 3-BPFA bridging molecules. The Zn···Zn distance is 8.618 Å for each rhombus side. The four iron centers are also coplanar and form a parallelogram with side distances of 5.498 and 17.391 Å, respectively. The eight metal centers assembled a chair-shape macrocyclic structure in an interval fashion, in which four zinc atoms form the seat and the two *syn*-ferrocenyl units and the two *anti*-ferrocenyl units form the back and legs of the chair, respectively. This structure also exists in complexes **8**−**11**. The corresponding parameters are listed in Table 3.

Although the van der Waals radii of a metal atom increases with atomic weight (Zn 1.39 Å[26]; Cd 1.58 Å[26]; Hg 1.75 Å[41]), the dimensions of the macrocyclic units are nearly identical with the alteration of the coordination metal. This observation suggests that two Cp-"arm" groups should have corresponding conformation change to adopt the similar size of the MOFs. This assumption is confirmed by the alteration of the corresponding dihedral angles between C_P planes, the C_P plane and pyridyl rings, and between two pyridyl rings of 3-BPFA (Supporting Information, Table S1). The distances of M^{II}-N_{py} in complexes **7**−**11** (Zn−N 2.228(2)−2.303(2) Å; Cd−N 2.346(5)−2.446(5) Å; Hg−N 2.530(3)−2.615(2) Å) clearly increase with the rise of the atomic radii (Zn→Cd→Hg), which are normal separates in similar metal complexes.[39,42]

Similar to dimers **4** and **5**, the two pyridyl planes of 3-BPFA in **7** have strong intramolecular $\pi\cdots\pi$ stacking interactions (centroid-to-centroid distance is 3.77 Å), which lead to a short $M^{II}\cdots M^{II}$ distance in the macrocyclic units. This interaction is also present in **8**−**11**. The corresponding parameters are listed in Table 4. In complex **7**, Zn_4 units link to each other through Zn−N bonding, creating a 2D network. Moreover, these Zn^{II} sheets are linked through two weak C−H···S interactions among the adjacent units. It has been reported that the existence of weak C−H···X (X = F, Cl, Br, I, O, S, and N) hydrogen-bonding interactions could partially provide driving forces for the alignment of complexes.[25,30,42,43] As a result, Zn−Fe MOFs adopt a "closely packed" fashion to form a three-dimensional architecture in an ···*AAA*··· stacking motif (Figure 10b).

Replacing the anion thiocyanate in **7** by using azide produces the Zn−Fe M′-MOFs **8**, and two complexes (**7** and **8**) have very similar structure. The geometric parameters of each Zn_4 unit in 2D networks of **8** are listed in Table 3. This structure similarity is also present in

(41) (a) Pyykko, P.; Straka, M. *Phys. Chem. Chem. Phys.* **2000**, *2*, 2489. (b) King, J. B.; Haneline, M. R.; Tsunoda, M.; Gabbai, F. P. *J. Am. Chem. Soc.* **2002**, *124*, 9350.

(42) Fleisher, H.; Dienes, Y.; Mathiasch, B.; Schmitt, V.; Schollmeyer, D. *Inorg. Chem.* **2005**, *44*, 8087–8096.

(43) (a) Dong, Y.-B.; Jin, G.-X.; Zhao, X.; Tang, B.; Huang, R.-Q. *Organometallics.* **2004**, *23*, 1604–1609. (b) Dong, Y.-B.; Jin, G.-X.; Smith, M. D.; Huang, R.-Q.; Tang, B.; zur Loye, H.-C. *Inorg. Chem.* **2002**, *41*, 4909–4914.

Table 4. Dihedral Angles (θ) and Centroid-to-Centroid Distances (d) between the Pyridyl Planes for 3-BPFA in Complexes **4**−**11** [deg and Å]

complex	θ [deg.]	d [Å]
3-BPFA	21.61	4.66
4	6.95	3.50
5	14.66	3.63
6[a]	0	4.27
7	18.77	3.77
8	17.26	3.73
9	18.09	3.73
10	15.25	3.78
11	19.49	3.67

[a] Two pyridyl planes from two different 3-BPFA in same macrocycle.

complexes **9**−**11**, although the different hydrogen bonding exist in **9**−**11** to connect adjacent M^{II} sheets and build three-dimensional architectures, instead of C−H···S hydrogen in **7** (see Supporting Information).

By using nitrate ion as counteranion, Cd−Fe M′-MOFs **10** was obtained. Different from other MOFs, the Cd^{II} center is coordinated by two water molecules instead of anions in **10**. The coordinated water molecules are located on both sides of the MOFs plane with the Cd−O distance of 2.354(5) Å. Nitrate ions fill in cavities of 2D layers and form hydrogen-bonding with coordination water molecules. This H-bonding results in an infinite water−anion "zigzag" chain (Figure 11). Thus, the $[H_2O(NO_3)]^-$ in **10** can be regarded as the analogue of the anion ligand.[44]

By using Hg^{II} ion as coordination center, Hg−Fe M′-MOFs **11** is obtained from methanol solution of 3-BPFA and $HgCl_2$. It is notable that in this reaction, the final product does not depend on the metal-to-ligand ratio in the preparation. The different metal-to-ligand ratios including 1:1, 1:2, and 1:3 were isolated as the only product, which is similar to the preparation of complex **6**. The significantly different structures in the two assembled mercury complexes (**6** and **11**) indicate the important roles of the anion ligands. Because of the bigger ionic radius and weaker coordination ability of Br^- anion relative to Cl^- anion, complexes with the Br^- anion incline to form the low-coordination sphere to the Hg^{II} ion. This phenomenon has been observed in many complexes previously,[45] and also extended to HgI_2 complexes.[39,42c,46]

Initially, self-assembly between 3-BPFA and Zn^{II}, Cd^{II}, and Hg^{II} salts is attempted to generate porous coordination networks, in which the desired cavities might be functionalized by the N−H group and O atom as a potential hydrogen donor and acceptor or coordination sites for guest inclusions. Nevertheless, the strong intramolecular $\pi\cdots\pi$ stacking leads to short $M^{II}\cdots M^{II}$ distances (~8.65 Å) in the MOFs, resulting in very limited space in the frameworks for guest molecules. Thus, no molecules were detected by crystallography in the cavities.

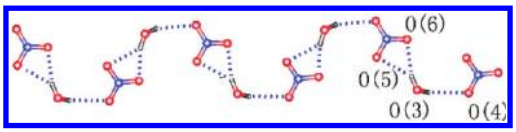

Figure 11. One-dimensional hydrogen-bonding chain between water molecules and nitrate ions in **10**. (H(3a)···O(4) 2.317 Å; H(3b)···O(6) 2.363 Å; H(3b)···O(5) 2.464 Å).

Discussion of Structural Properties. We have demonstrated that organometallic two-"arms" ligand 3-BPFA, with intermolecular bonding capacity, can be used as a "*preconstructed building block*" to prepare mixed-metal structures. The various assemblies were constructed by manipulating the two equivalent flexible "arms" of ligand 3-BPFA. The helical supramolecular array of free ligand 3-BPFA results from intermolecular hydrogen bonds, which induces the slight rotation of two Cp rings. Because of strong hydrogen-bonding interactions, the pyridyl nitrogen atoms of 3-BPFA adopt an outward fashion conformation (Figure 12a). In cage-type structures **1**−**3**, two Cp-"arm" units occur to highly twisted interleaving owing to the strong coordination to Cu^{II}, Co^{II}, and Ni^{II} metal centers, which results in two N_{Py} atoms bonding to metal centers in an inward fashion (Figure 12b). In dimers **4** and **5**, the interactions of metal−metal and $\pi\cdots\pi$ stacking induce two nearly parallel pyridyl planes, which adopt a "head-to-head" fashion to bond Ag atoms (Figure 12c-d). In macrocycle **6**, although there are strong intramolecular hydrogen-bonding interactions, the highly distorted interleaving of the two "arms" is still constructed because of the big radius of Hg^{II} and the tetra-coordination geometry. Similar to the coordination mode of **4** and **5**, two pyridyl nitrogen atoms in **6** are still in the same orientation (Figure 12e). In MOFs **7**−**11**, Cp-"arm" planes are nearly parallel, resulting in strong $\pi\cdots\pi$ stacking interaction of pyridyl rings in 3-BPFA. Different from **4**−**6**, two pyridyl rings of 3-BPFA in complex **7**−**11** adopt an opposite binding mode to two different d^{10} metal centers (Figure 12f), which results in a hexa-coordination geometry and constructs a series of 2D MOFs. However, the complete *trans*-conformation (Scheme 3), which has two Cp-"arm" units in opposite directions, is not formed in this series of M-3-BPFA complexes. This is likely due to the $\pi\cdots\pi$ stacking interaction of 3-BPFA tending to the steady 2D structures.

In this series of processes, the transformation of dihedral angles between Cp rings and relative pyridyl rings is consistent with the change of the corresponding structures. The conformational parameters for complexes **1**−**11** are listed in Supporting Information, Table S1. Apparently, the flexible "spacers" carry out flexible "assembling" to construct structural versatility.

Properties and Spectra Analysis. The IR spectrum of the free ligand displays the characteristic strong $\nu_{C=O}$ band around 1644 cm^{-1}, corroborating the −CONH− functional group in 3-BPFA. The $\nu_{C=O}$ vibrations are red-shifted (ranging from 1646 to 1672 cm^{-1}) in complexes **1**−**11** relative to the free ligand. This shift may

(44) (a) Zhang, X.-M.; Tong, M.-L.; Chen, X.-M. *Angew. Chem., Int. Ed.* **2002**, *41*, 1029–1031. (b) Zhang, X.-M.; Tong, M.-L.; Gong, M.-L.; Lee, H.-K.; Luo, L.; Li, K.-F.; Tong, Y.-X.; Chen, X.-M. *Chem.—Eur. J.* **2002**, *8*, 3187–3194. (c) Grossel, M. C.; Dwyer, A. N.; Hursthouse, M. B.; Orton, J. B. *CrystEngComm* **2007**, *9*, 207–210. (d) Wilson, A. J. *Soft Matter* **2007**, *3*, 409–425.

(45) (a) Lee, C.-J.; Huang, C.-H.; Wei, H.-H.; Liu, Y.-H.; Lee, G.-H.; Wang, Y. *J. Chem. Soc., Dalton Trans.* **1998**, 171–176. (b) Matthews, C. J.; Clegg, W.; Heath, S. L.; Martin, N. C.; Stuart Hill, M. N.; Lockhart, J. C. *Inorg. Chem.* **1998**, *37*, 199–207. (c) Bell, N. A.; Goldstein, M.; March, L. A.; Nowell, I. W. *J. Chem. Soc., Dalton Trans.* **1984**, 1621–1624. (d) Morsali, A.; Masoomi, M. Y. *Coord. Chem. Rev.* **2009**, *253*, 1882–1905.

(46) Bharara, M. S.; Parkin, S.; Atwood, D. A. *Inorg. Chem.* **2006**, *45*, 2112–2118.

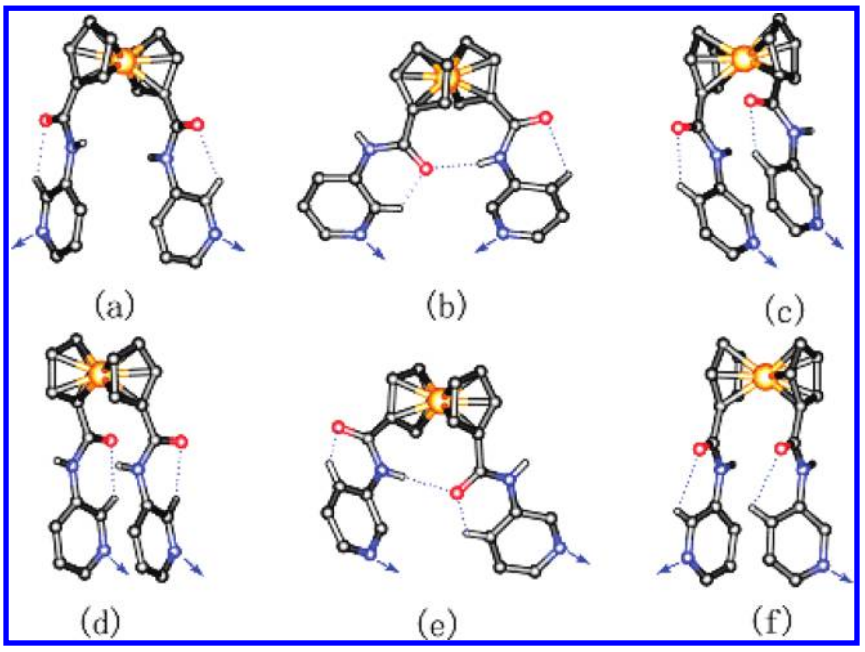

Figure 12. Various conformations and intramolecular H-bonding patterns of two Cp-"arm" units for 3-BPFA in different complexes.

result from the interactions in the complexes, including $N_{Py}\rightarrow M$ coordination and different intra- or/and intermolecular hydrogen bonding. Similar shifts of $\nu_{C=O}$ upon coordination have been observed in other complexes previously.[9,47]

Crystals of complexes **4**−**11** are stable in air at room temperature for a considerable length of time. The UV−vis spectra of ligand 3-BPFA and corresponding complexes **4**−**11** are determined in DMF solutions (Figure 13). The strong absorption around 275 nm may be attributed to the metal−ligand charge transfer (MLCT) transitions; a similar absorption was observed in 1,1′-bis[(4-pyridylamino)carbonyl]ferrocene (4-BPFA) complexes.[9a] The characteristic absorptions of ferrocene from the $^1E_{1g}\leftarrow{}^1A_{1g}$ transition exhibit weak absorption around 440 nm.[9,48]

The differential pulse voltammetry (DPV) technique is employed to obtain well-resolved potential information. The redox properties of the free ligand 3-BPFA and complexes **4**−**11** are investigated in DMF. DPV data are listed in Table 5. The ligand 3-BPFA ($E_{1/2}$ = 360 mV from DPV relative to that of Fc/Fc^+, as shown in Figure 14) is more difficult to oxidize than the unsubstituted parent ferrocene, which is probably due to the electron-withdrawing property of the substituent amide groups on Cp rings.

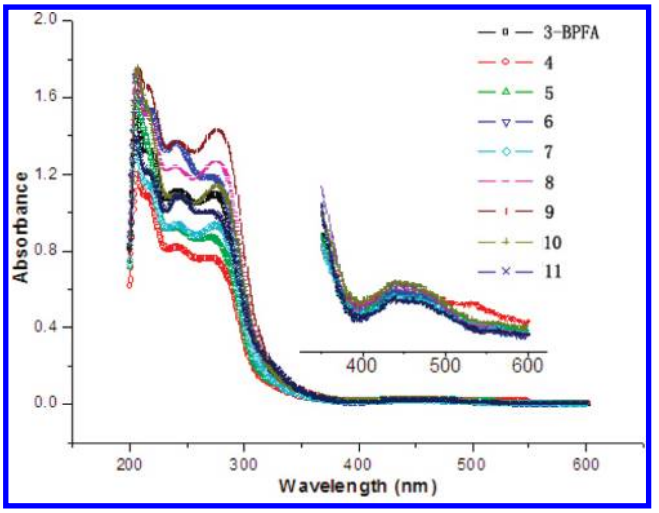

Figure 13. UV−visible absorption spectra at ambient temperature in MeOH (2.5×10^{-5} M) for the ligand 3-BPFA and in MeOH (2.5×10^{-5} M) complexes **4**−**11**.

The properties of multinuclear mixed-valence complexes have been extensively investigated because of their potential applications, for example, as solar energy conversion catalysts, photoinduced magnetic memory devices, chemical sensors, nanoscale switches, and molecular-scale rectifiers.[49] DPV results show that the silver(I) complexes **4** and **5** exhibit one peak at 0.836 and 0.828 V, respectively, corresponding to the one-electron metal-based oxidation Fc/Fc^+, suggesting no communication between the two ferrocene units in dimers **4** and **5** in DMF solution. The peaks corresponding to Ag/Ag^+ oxidation in **4** and **5** appear at 0.412 and 0.440 V, respectively. Macrocycle **6** exhibits only one redox peak at 0.868 V, which reveals the absence of ferrocene-ferrocene interactions in tetrametal unit.

(47) Carr, J. D.; Coles, S. J.; Hursthouse, M. B.; Tucker, J. H. R. *J. Organomet. Chem.* **2001**, *637*, 304–310.
(48) (a) Sohn, Y. S.; Hendrickson, D. N.; Gray, H. B. *J. Am. Chem. Soc.* **1971**, *93*, 3603–3612. (b) Armstrong, A. T.; Smith, A. T.; Elder, E.; McGlynn, S. P. *J. Chem. Phys.* **1967**, *46*, 4321–4328.
(49) (a) Fehlhammer, W. P.; Fritz, M. *Chem. Rev.* **1993**, *93*, 1243–1280. (b) Han, G.; Guo, D.; Duan, C.-Y.; Meng, Q. J. *New J. Chem.* **2002**, *26*, 1371–1377. (c) Feig, A. L.; Lippard, S. J. *Chem. Rev.* **1994**, *94*, 759–805. (d) Piepho, S. B. *J. Am. Chem. Soc.* **1990**, *112*, 4197–4206. (e) Taft, K. L.; Papaefthymiou, G. C. *Science* **1993**, *259*, 1302–1305. (f) Beley, M.; Chodorowski, S.; Collin, J. P. *Angew. Chem., Int. Ed. Engl.* **1994**, *33*, 1775–1778. (g) Ferretti, A.; Lami, A.; Ondrechen, M. J.; Villani, G. *J. Phys. Chem.* **1995**, *99*, 10484–10491. (h) Bublitz, G. U.; Laidlaw, W. M.; Denning, R. G.; Boxer, S. G. *J. Am. Chem. Soc.* **1998**, *120*, 6068–6075. (i) Guo, D.; Qian, C.-Q.; Duan, C.-Y.; Pang, K.-P.; Meng, Q.-J. *Inorg. Chem.* **2003**, *42*, 2024–2031. (j) Guo, D.; Han, G.; Duan, C.-Y.; Pang, K.-L.; Meng, Q. J. *Chem.Commun.* **2002**, 1096–1097. (k) Roy, S.; Sarkar, B.; Duboc, C.; Fiedler, J.; Sarper, O.; Lissner, F.; Mobin, S. M.; Lahiri, G. K.; Kaim, W. *Chem.—Eur. J.* **2009**, *15*, 6932–6939.

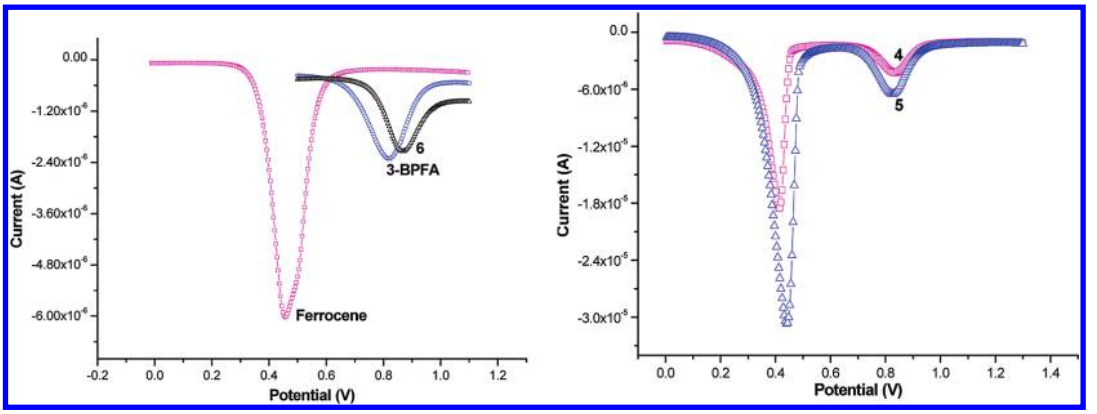

Figure 14. DPV of (left) ferrocene, **3-BPFA**, **6**, and (right) **4**−**5** in DMF (0.1 M n-Bu_4NClO_4); concentration: 0.5×10^{-3} M, pulse height 50 mV, pulse width 25 ms.

Table 5. Differential Pulse Voltammetric Responses of **3-BPFA** and **4**−**11** in DMF Containing n-Bu_4NPF_6 (0.1 M)[a]

	DPV	
compound	*Ep* [mV]	$E_{1/2}$ [mV, vs Fc/Fc^+]
Ferrocene	456	0
3-BPFA	816	360
4	836	380
	412	/
5	828	372
	440	/
6	868	412
7	832	376
8	828	372
9	836	380
10	860	404
11	860	404

[a] Ferrocene as external standard, vs Ag/Ag^+.

The measurements of solution-state DPV of polymers **7**−**11** are shown in Figure 15. The results demonstrated that all these polymers show a single peak, which can be assigned to the one-electron-transfer process of the ferrocenyl moiety. The half-wave potential for complexes are ($E_{1/2}$ vs that of Fc/Fc^+) 0.376 V (**7**), 0.372 V (**8**), 0.380 V (**9**), 0.404 V (**10**), and 0.404 V (**11**). Relative to free ligand 3-BPFA, the half-wave potentials of **4**−**11** are all slightly shifted to higher potential. It can be envisaged that the potential increase of Fc in the complexes is caused by the coordination to the central metal ions, which withdraws electrons from the ligand and makes the ferrocene unit more difficulty to oxidize.[50] This observation is consistent with the previous results of transition metal−ferrocenyl systems.[9,13,51] On the basis of the "charging effects" by Bard[52], the narrow lines of Figure 15 likely indicate that

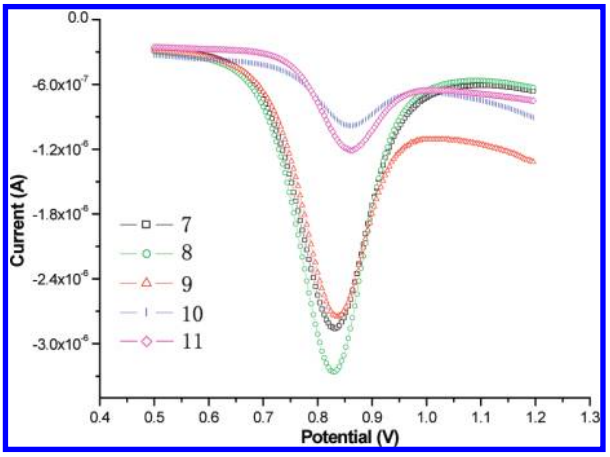

Figure 15. DPV of complexes **7**−**11** in DMF (0.1 M n-Bu_4NClO_4); concentration: 0.5×10^{-3} M, pulse height 50 mV, pulse width 25 ms.

the 2D MOFs **7**−**11** dissociate to oligomers and even monomers in DMF solution.

Conclusions

The present work demonstrates that a simple complex module can be pertinently assembled to various desired architectures via the flexible molecular arms. This synthetic strategy, using flexible arm-like ligands to construct differently molecular architectures, could be applied in producing higher diversity of supermolecular structures.

The complex module 3-BPFA is so flexible that it can vary the shape and the dimensionality of the assemblies by changing the dihedral angles and the metal-coordination mode of the 3-BPFA (*syn*- and *anti*- configuration and/or *cis*- and *trans*-conformation). (Schemes 2, 3) Consequently, the "building block" 3-BPFA generates a large variety of assembled structures: (a) helical chains, (type I motif in Scheme 2); (b) molecular cage and capsules (**1**, **2**, and **3**, type II motif in Scheme 2); (c) dimers and molecular macrocycle (**4**, **5**, and **6**, type III motif in Scheme 2); (d) mixed-MOFs (**7**−**11**, type IV motif in Scheme 2). Thus, the control of these features is one of the key factors to develop a pertinent synthesis strategy for the desired architectures from a simple building block with molecular arms.

The properties of metal ions mediate the tuning of the structures of complexes and the conformation of the two arms. Copper(II), cobalt(II), and nickel(II) ions have small

(50) Barranco, E. M.; Crespo, O.; Gimeno, M. C.; Jones, P. G.; Laguna, A.; Sarroca, C. *J. Chem. Soc., Dalton Trans.* **2001**, 2523–2529.
(51) (a) Zheng, G. L.; Ma, J. F.; Su, Z. M.; Yan, L. K.; Yang, J.; Li, Y. Y.; Liu, J. F. *Angew. Chem., Int. Ed.* **2004**, *43*, 2409–2411. (b) Horikoshi, R.; Mochida, T.; Moriyama, H. *Inorg. Chem.* **2002**, *41*, 3017–3024. (c) Ion, A.; Buda, M.; Moutet, J. C.; Saint-Aman, E.; Royal, G.; Gautier-Luneau, I.; Bonin, M.; Ziessel, R. *Eur. J. Inorg. Chem.* **2002**, 1357–1366. (d) Duan, C. Y.; Tian, Y. P.; Liu, Z. H.; You, X. Z.; Mak, T. C.W. *J. Organomet. Chem.* **1998**, *570*, 155–162. (e) Barranco, E. M.; Crespo, O.; Gimeno, M. C.; Jones, P. G.; Laguna, A.; Villacampa, M. D. *J. Organomet. Chem.* **1999**, *592*, 258–264. (f) Xu, Y. M.; Saweczko, P.; Kraatz, H. B. *J. Organomet. Chem.* **2001**, *637*, 335–342.
(52) Hubbard, A. T.; Anson, F. C. In *Electroanalytical Chemistry*; Bard, A. J., Ed.; Marcel Dekker: New York, 1970; Vol. *4*, pp 129−214.

ionic radii and unsaturated d-orbital electronic configuration. The cavity assembly of **1** is due to the five coordination geometry of the copper(II) ion. Whereas for **2** and **3** the encapsulated anion is an essential part of the structures to achieve six coordination saturated geometry of Ni^{II} and Co^{II}. The "soft" silver(I) ion with d^{10} electronic configuration forms dimers because of the variation of coordination geometry, while zinc(II), cadmium(II), and mercury(II) ions, which have d^{10} electronic configuration and have much stronger tendency to display six-coordination geometry, have saturated coordination and form 2D MOFs. Besides the above factors, the structure of complexes can also be influenced by anion coordinations. Therefore, the structures of the motifs can be described as the result of reading molecular information stored in the ligand by the metal ions and/or counteranions. Furthermore, noncovalent interactions (such as, hydrogen bonding, π stacking, and cation$\cdots\pi$ interactions) increase the dimensionality of the system. Thus the selection of the solvent and anions result in further subtle structural variation in the crystal structure.

In summary, the conformational flexibility of the arm-like bridging ligand 3-BPFA allows the conformational change of the architecture in the bimetallic assemblies.

Acknowledgment. This work was supported by the National Natural Science Foundation of China (No. 20873135 to Y.L.;No. 50903081 to K.W.), the China Postdoctoral Science Foundation (No. 20070420724 to K.W.), the Cultivation Fund of the Key Scientific and Technical Innovation Project, Ministry of Education of China (No. 707036) and the Natural Science Foundation of Jiangsu Province (NO. BK2008579 to K.W.).

Supporting Information Available: Some figures and tables, as well as crystallographic data. This material is available free of charge via the Internet at http://pubs.acs.org.